Hindawi
International Journal of Chemical Engineering
Volume 2023, Article ID 8691957, 20 pages
https://doi.org/10.1155/2023/8691957

Research Article

Screening of Pure ILs and DESs for CO_2 Separation, N_2O Separation, and H_2S Separation Processes

Yingying Zhang,[1,2,3] **Xuzhao Yang**,[1,2,3] **Jingli Han**,[1,3] **Junfeng Tian**,[1] **Ting Zhang**,[1] **Yakun Li**,[1,2,3] **Jiangqiang Zhang**,[1,2,3] **Yuxin Shi**,[1] **and Jingjing Zhang**[1]

[1]*Department of Material and Chemical Engineering, Zhengzhou University of Light Industry, Zhengzhou 450002, China*
[2]*Henan Engineering Research Center of Catalysis and Seperation of Cyclohexanol, Zhengzhou University of Light Industry, Zhengzhou 450002, China*
[3]*Zhengzhou Key Laboratory of Fine Chemicals, Zhengzhou 450002, Henan, China*

Correspondence should be addressed to Yingying Zhang; zhangyy@zzuli.edu.cn and Xuzhao Yang; yangxz@zzuli.edu.cn

Received 21 August 2022; Revised 27 December 2022; Accepted 30 December 2022; Published 18 February 2023

Academic Editor: Pedro Castano

Ionic liquids (ILs) are proposed as potential "green" solvents with remarkable properties. Deep eutectic solvents (DESs) are a new type of ILs with additional properties, such as higher biodegradability and a lower price. ILs and DESs are "green" absorbents for various gas separations, such as CO_2/N_2, $CO_2/H_2/CO$, H_2S/CH_4, and N_2O/N_2. Due to their large number, the screening of ILs is crucial. Although ILs with high absorption capacities were screened using gas solubility and selectivity, it is important to consider the energy and solvents used in the process. In this paper, the absorbent amount and the energy consumption were used for screening absorbents for various gas separation processes. The results reveal that physical IL [Bmim][DCA] and chemical IL [Eeim][Ac] are screened for CO_2/N_2 and $CO_2/H_2/CO$ separation, physical IL [Omim][PF_6] for H_2S/CH_4 separation, and physical IL [P_{66614}][eFAP] for NO/N_2 separation. The screened ILs offer some advantages over commercial absorbents in terms of lower energy consumption or amount.

1. Introduction

Every year, large amounts of gases are emitted into the atmosphere, with CO_2 being the primary greenhouse gas [1, 2], N_2O having a potential impact on global warming that is 310 times greater than that of CO_2 [3], and H_2S being one of the highest sulfur-containing compounds. Excess emissions of CO_2 and N_2O result in global warming and climate change, while H_2S emissions result in acid rain. Therefore, it is necessary to identify effective measures to mitigate the emission of CO_2, N_2O, and H_2S from different sources.

Carbon capture and storage (CCS) can be used to reduce CO_2 emissions. Meanwhile, biomass syngas from biomass gasification is used in transportation as biofuels. CO_2 separation is required for CCS and biomass syngas purification. The current CO_2 separation technologies have several shortcomings, such as high energy consumption [4], corrosion degradation, and/or large-scale operations, which affect removal efficiency.

The primary sources of anthropogenic N_2O emissions are nylon production, nitric acid production, and vehicle exhaust emissions. Many N_2O emission reduction technologies have been developed, such as thermal decomposition and catalytic decomposition. However, they may be constrained by the large energy consumption and increasing CO_2 emissions.

There are several technologies for H_2S separation, such as absorption, oxidation, and adsorption [5]. Absorption technology is extensively used for H_2S separation, whereas aqueous alkanolamine solutions are currently employed in industrial natural gas treatment and sweetening plants [6]. However, the application of H_2S absorption technology is impacted, similar to CO_2 separation, by intensive energy consumption and/or large-scale operations.

Therefore, new gas separation processes for CO_2, N_2O, and H_2S must be developed to curb climate change and protect the environment. Ionic liquids exhibit remarkable properties for gas separation, such as high solubility for CO_2, N_2O, and H_2S. Although ILs have been used in studies related to gas separation [7–10], the large-scale commercial usage of ILs is limited by their high toxicity, poor biodegradability, and high cost. Deep eutectic solvents have low toxicity, biodegradability, and low cost and are proposed as promising CO_2 absorbents [11–14].

In our previous work, Gibbs free energy change (ΔG) was employed to evaluate the performance of solvents [15, 16] for separating CO_2 from biogas and NH_3 from synthetic ammonia purge gas [17]. However, the effective absorbents for various gas streams with different conditions were not determined. In this study, thermodynamic analysis was utilized for gas separation using pure ILs and DESs. For CO_2 streams, effluent gases, kiln gas, and biomass syngas were chosen. For the H_2S stream, high-sulfur natural gas was chosen. For the N_2O stream, adipic acid off-gas was chosen. For various gas streams, several absorbents were screened as potential gas absorbents. Furthermore, the relationship between the performances, the properties, and the critical properties of gas streams was investigated. All of these are employed in the development of new gas separation technologies.

2. Gas Separation and Thermodynamic Model

2.1. Gas Streams. In this work, effluent gases were chosen as CO_2 streams due to their large emission amounts and low CO_2 concentration, whereas kiln gas was chosen due to its high CO_2 concentration. Biomass syngas is chosen as the CO_2 stream for $CO_2/CO/H_2$. The high-sulfur natural gas is used as the H_2S stream for H_2S/CH_4, and the adipic acid off-gas is used as the N_2O stream for N_2O/N_2. Table 1 lists the typical conditions of different gas streams.

2.2. Gas Separation Process. The gas separation process using liquid absorbents is shown in Figure 1. The absorbent quantity (m_{abs}, g abs·g X^{-1}) can be calculated using the following equation:

$$m_{\text{abs}} = \frac{M_{abs}}{M_x}\frac{(1-x_s)(1-x_a)}{x_a - x_s}, \tag{1}$$

where M_{abs} and M_x are the molecular weights of the absorbent and X gas, respectively, and g·mol^{-1}. x_a and x_s are the molar ratios of the X gas in the absorption tower and desorber, respectively.

The energy consumption required in the gas separation process can be calculated as shown in

$$\begin{aligned} Q_{\text{tot}} &= Q_{\text{des}} + Q_{\text{sens}} + W_{\text{comp}} \\ &= -\frac{n_x}{M_x}R\left(\frac{\partial \ln H_x}{\partial (1/T)}\right) + \frac{nRT}{M_x}\ln\left(\frac{P_a}{P_1}\right) + \frac{1}{M_x}n_{abs}C_{p,abs}(T_s - T_a), \end{aligned} \tag{2}$$

where n_x denotes the molecular weight of the X gas in moles. H_x denotes the Henry constant of X gas in the absorbents in bar units. P_a and P_1 denote the pressure of the absorption tower and the initial pressure, respectively, in bar units. $C_{p,\text{abs}}$ represents the isobaric heat capacities of the absorbents in J·mol^{-1}·K^{-1}. T_a and T_s denote the temperatures of the absorption tower and desorber, respectively.

2.3. Theory. In thermodynamics, ΔG was used as the evaluation criteria to determine if the isothermal reversible process was spontaneous. As shown in Figure 2, the separation process is nonspontaneous, and the Gibbs free energy change for System 1 is above zero ($\Delta G_1 > 0$). Six reversible processes were designed, and the summation is represented as ΔG_2 for Surrounding 2. System 3 is composed of System 1 and Surrounding 2. Moreover, the addition of energy and absorbents causes ΔG_2 to be negative. In Figure 2, ΔG_{comp} represents the isothermal reversible compression process, ΔG_{abs} represents the reversible absorption process of X absorption, ΔG_T represents the reversible adiabatic expansion and reversible temperature increasing process of the solution, ΔG_{des} represents the reversible X gas desorption process, ΔG_{exp} represents the isothermal reversible expansion of the other gas, and ΔG_T' represents the reversible adiabatic expansion and the reversible isothermal compression of the X gas. The optimal operating conditions are achieved when ΔG_3 is equal to 0, and the performance of different absorbents can be evaluated. Therefore, using the thermodynamic analysis as proposed in our previous work, the number of absorbents and the energy consumption are combined by Gibbs free energy change [12, 13].

ΔG for different systems and processes can be calculated using the equations given in equations (3)–(10).

$$\Delta G_3 = \Delta G_1 + \Delta G_2, \tag{3}$$

$$\Delta G_1 = -nRT\sum_{i=0}^{N} y_i \ln y_i, \tag{4}$$

$$\begin{aligned} \Delta G_2 = {} & \Delta G_{\text{comp}} + \Delta G_{\text{abs}} + \Delta G_{\text{sens}} + \Delta G_{\text{des}} \\ & + \Delta G_{\text{exp}} + \Delta G_T', \end{aligned} \tag{5}$$

where n is the number of moles in the gas stream, and y_i represents the molar fraction of component i in the stream.

Table 1: The typical condition of gas streams.

Condition	Biomass syngas [18]	Effluent gases [19]	Kiln gas [20, 21]	High-sulfur natural gas [22]	Adipic acid off-gas [23]
T_a (K)	423.15	423.15	423.15	298.15	298.15
P_a (bar)	1	1	1	1	1
T_s (K)	298.15	298.15	298.15	298.15	298.15
P_s (bar)	1	1	1	1	1
y_{CO_2}	0.30	0.12	0.25		
y_{N_2}	—	0.88	0.75		0.55
y_{CH_4}	—	—	—	0.68	
y_{N_2O}					0.45
y_{H_2S}				0.32	
y_{CO}	0.30	—	—		
y_{H_2}	0.40	—	—		

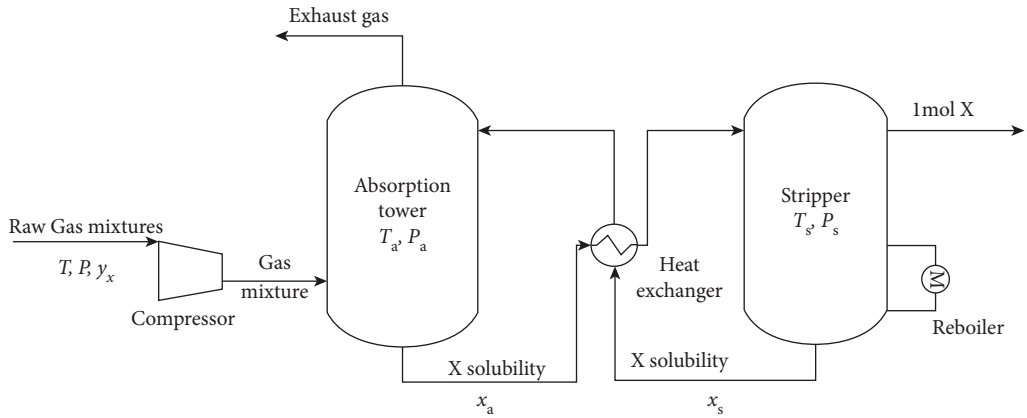

Figure 1: Reduced engineering flow sheet for gas separation process.

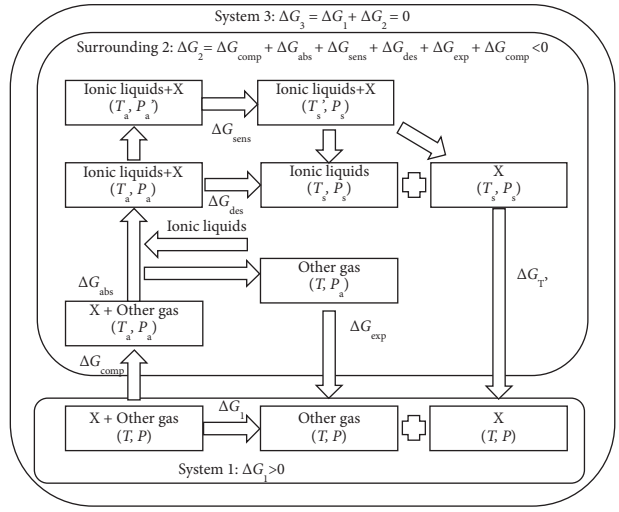

Figure 2: The thermodynamic analysis of the coupling process of gas separation with absorbents.

$$\Delta G_{\text{comp}} = \sum_{i=0}^{N} n y_i G_i^g (T_a, P_a) - \sum_{i=0}^{N} n y_i G_i^g (T, P), \quad (6)$$

where $G_i^g(T, P)$ and $G_i^g(T_a, P_a)$ are the G values of the gaseous component i at (T, P) and (T_a, P_a), respectively, and they are calculated using the formula $G = H - TS$. The NIST standard reference database provides the values of H and S for the gas components.

$$\Delta G_{\text{abs}} = n y_x R T_a [\ln H_x + \ln K_x], \quad (7)$$

$$\Delta G_{\text{des}} = -n y_x R T_s [\ln H_x + \ln K_x], \quad (8)$$

where H_x denotes Henry's constant and K_x denotes the chemical reaction constant of X gas in absorbents.

$$\begin{aligned}
\Delta G_T &= \sum_{j=0}^{N} n_{abs} x_j G_j^l (T_s, P_s, x_s) - \sum_{j=0}^{N} n_{abs} x_j G_j^l (T_a, P_a, x_a) \\
&= \sum_{j=0}^{N} n_{abs} x_j \left\{ \begin{array}{l} \left[\left(\Delta_f H_{j,298.15K}^l + \int_{298.15K}^{T_s} C_{p,j}^l dT \right) - T_s \times \left(S_j^l (298.15K) + \int_{298.15K}^{T_s} \frac{C_{p,j}^l}{T} dT \right) \right] \\ - \left[\left(\Delta_f H_{j,298.15K}^l + \int_{298.15K}^{T_a} C_{p,j}^l dT \right) - T_a \times \left(S_j^l (298.15K) + \int_{298.15K}^{T_a} \frac{C_{p,j}^l}{T} dT \right) \right] \end{array} \right\} \\
&= \sum_{j=0}^{N} n_{abs} x_j \left[\int_{T_a}^{T_s} C_{p,j}^{abs} dT \right] - (T_s - T_a) \times S_j^{\text{abs}} (298.15K) - \left(T_s \int_{298.15K}^{T_s} \frac{C_{p,j}^{abs}}{T} dT - T_a \int_{298.15K}^{T_a} \frac{C_{p,j}^{abs}}{T} dT \right),
\end{aligned} \quad (9)$$

where $\Delta_f H_j$, 298.15 K represents the standard enthalpy change in the formation of j in the absorbents at 298.15 K; S_j (298.15 K) represents the standard molar entropy of j at 298.15 K; and $C_{p,j}$ represents the isobaric heat capacity of j in the absorbents.

$$\Delta G_{\text{exp}} = \sum_{i=0}^{N} n y_x G_x^g (T, P) - \sum_{i=0}^{N} n y_x G_x^g (T_a, y_x P_a), \quad (10)$$

where y_x is the mole fraction of X gas in the gas stream, G_i^g $(T_a y_x P_a)$ is the G value of the gaseous component i at $(T_a, y_x P_a)$.

$$\Delta G_T' = \sum_{i=0}^{N} n y_i G_i^g (T, P) - \sum_{i=0}^{N} n y_i G_i^g (T_s, P_s), \quad (11)$$

where $G_i^g(T_s, P_s)$ is the G value of the gaseous component i at (T_s, P_s).

3. The Properties of Absorbents

The properties of liquid absorbents, including Henry's law constants of different gases in ILs/DESs, reaction equilibrium constants, the density of ILs/DESs at 298.15 K, and the heat capacity of the ILs/DESs, have been collected and listed in Table 2. In conventional ILs/DESs, the uncertainty in Henry's law constants of CO_2, H_2S, and N_2O was estimated to be ±8 bar, ±0.4 bar, and ±0.07 bar, respectively. Henry's law constants and reaction equilibrium constants were correlated for some physical ILs and the chemical ILs/DESs as per the CO_2 solubility data described in our previous work [11]. The uncertainties in the densities and the heat capacities of the conventional ILs/DESs were ±63 J·mol^{-1}·K^{-1} and ±13 g·cm^{-3}, respectively, based on the experimental data presented in Table 2. The names and molar weights of absorbents are listed in Appendix A (Supplementary data available here).

4. Results and Discussion

The desorption temperatures of absorbents in this study are identical to those in our previous work [12], which are 299.15–323.15 K for physical absorbents, 299.15–345.15 K, and 299.15–353.15 K for chemical DES and ILs, respectively. The absorption pressure is iterated until $\Delta G_3 = 0$, and the optimal conditions, absorbent amount, and energy consumption are obtained.

4.1. Analysis of Gas Absorbents

4.1.1. Absorption Pressure. As shown in Figures 3 and 4, [BmPy][FAP] represents the minimum P_a, which is 16.16–87.77 bar, 8.75–45.65 bar, and 7.66–44.98 bar in 299.15–323.15 K for effluent gases, kiln gas, and biomass syngas, respectively. Among the four chemical absorbents that were analyzed, [Eeim][Ac] exhibits the lowest absorption pressures for the three CO_2 streams, with values of 70.60–137.96 bar, 36.00–74.44 bar, and 41.98–123.37 bar within 315.15–345.15 K, respectively. Among the ten physical absorbents that were analyzed for N_2O/N_2 separation, [Omim][PF_6] exhibits the lowest value of P_a in the temperature range of 299.15–323.15 K with pressure values in the range of 3.97–13.49 bar. [Bmim][FAP] exhibits the

Table 2: Henry's constant of X gas (H_x) in physical absorbents, the density at 298.15 K ($\rho_{298.15}$), and the isobaric heat capacity (C_p) of CO_2 absorbents.

Absorbents	T (K)	H_x (bar)	K_x	$\rho_{298.15}$ (g·cm^{-3})	C_p (J·mol^{-1}·K^{-1})
CO_2 absorbents					
[Emim][BF_4]	298.1–343.0	81.1–162.1 [24]		1.283 [25–27]	308.1–324.5 [28–31]
[C_2OHmim][BF_4]	303.2–353.2	108.0–198.0 [32]		1.330 [33, 34]	439.0–475.0 [28]
[Emim][PF_6]	303.2–343.2	61.2–138.7 [11]		1.468 [35]	350.0–368.4 [36]
[Emim][NTf_2]	283.1–343.1	25.3–77.1 [37, 38]		1.518 [39–41]	501.2–530.4 [28, 42, 43]
[Emmim][NTf_2]	283.1–323.1	28.6–60.5 [37]		1.487 [44]	481.4–498.8 [44]
[Emim][OTf]	303.2–343.2	83.0–158.4 [11]		1.385 [45–47]	380.1–394.6 [48]
[Emim][$EtSO_4$]	283.3–343.1	62.1–184.7 [11]		1.237 [49, 50]	365.0–411.0 [51]
[Emim][Et_2PO_4]	313.2–333.2	69.9–96.6 [52]		1.145 [53]	470.0–486.0 [54]
[Bmim][BF_4]	283.1–344.3	40.8–123.4 [37, 55]		1.201 [56]	357.8–386.3 [57]
[Bmim][PF_6]	283.1–348.2	38.7–121.1 [58]		1.367 [59]	398.5–435.1 [60]
[Bmim][NTf_2]	293.1–323.1	29.0–49.1 [61]		1.436 [62]	564.1–581.7 [60]
[Bmim][DCA]	298.2–333.3	71.9–102.3 [11]		1.060 [63]	376.6–389.3 [64]
[Bmim][TFA]	298.2–333.4	57.2–90.0 [11]		1.216 [65]	407.9–424.9 [66]
[Bmim][CH_3SO_4]	293.2–413.2	74.5–335.8 [11]		1.208 [67]	373.0–424.3 [68]
[Bmim][$OcSO_4$]	313.2–343.2	64.8–94.0 [11]		1.068 [40]	655.4–696.5 [69]
[Hmim][BF_4]	307.5–322.2	62.6–86.2 [70]		1.145 [71]	435.9–443.4 [72]
[Hmim][PF_6]	298.2–323.2	49.0–80.6 [11]		1.291 [73]	423.5–438.7 [74]
[Hmim][NTf_2]	293.2–413.2	27.8–122.4 [75]		1.372 [76]	626.2–704.0 [28]
[Omim][BF_4]	303.0–323.0	53.9–75.6 [61]		1.103 [71]	501.3–513.6 [77]
[Omim][NTf_2]	303.2–353.2	26.0–44.2 [11]		1.321 [65]	741.0–817.0 [28]
[C_{12} mim][NTf_2]	298.2–323.2	32.0–42.0 [11]		1.278 [78]	755.3–774.9 [79]
[BmPy][FAP]	303.2–343.2	25.7–46.1 [11]		1.583 [80]	773.0–803.0 [28]
[BmPy][NTf_2]	303.8–344.2	36.6–67.8 [11]		1.394 [81]	592.2–620.0 [32]
[Bmpy][OTf]	303.4–373.2	40.2–205.6 [11]		1.253 [82]	437.8–497.1 [82]
[Bpy][NTf_2]	298.2–333.2	32.0–51.7 [83]		1.448 [84]	581.5–597.6 [59]
[Hmpy][NTf_2]	283.2–333.2	25.4–46.2 [11]		1.362 [85]	612.1–652.1 [86]
[N_{4111}][NTf_2]	282.9–343.0	23.8–70.0 [11]		1.392 [87]	550.2–586.2 [88]
ChCl/urea (1 : 2)	313.0–333.0	123.0–182.0 [89]		1.360 [90–92]	183.2–186.4 [93]
ChCl/EG (1 : 2)	303.2–343.2	243.6–600.5 [94]		1.117 [95]	190.8–202.1 [93]
ChCl/Gly (1 : 2)	303.2–343.2	120.0–344.9 [96]		1.191 [95, 97]	237.7–250.3 [93]
[Emim][Ac]	298.1–348.1	4.3–6.3 [11]	285.0–808.0 [11]	1.099 [98]	322.6–343.0 [99]
[Eeim][Ac]	283.1–348.1	4.3–6.3 [11]	140.0–18.0 [11]	1.076 [100]	442.6–491.8 [99]
[Bmim][Ac]	298.1–348.1	4.0–7.0 [11]	167.0–39.0 [11]	1.052 [101]	381.0–414.0 [66]
Cho[Pro]/PEG200(1 : 2)	298.1–348.1	2.8–3.3 [12, 102]	1.3–1.6 [12, 102]	1.330 [103]	358.3–380.4 [102]
N_2O absorbents					
[Bmpy][FAP]	303.1–343.2	0.023–0.042 [104]		1.583 [105]	799.0–812.0 [106]
[P_{66614}][FAP]	303.1–343.2	0.043–0.070 [104]		1.182 [80]	1540.0–1580.0 [107]
[Bmim][FAP]	303.1–343.2	0.026–0.042 [108]		1.624 [109]	737.3–757.8 [110]
[Hmim][FAP]	303.1–343.3	0.022–0.043 [108]		1.550 [111]	764.0–781.2 [74]
[Bmim][NTf2]	298.0–348.0	0.002–0.404 [112]		1.437 [113]	589.1–600.3 [114]
[Bmim][BF_4]	298.0–348.0	0.001–0.208 [112]		1.201 [115]	385.6–394.9 [77]
[Bmim][DCA]	293.0–348.0	0.001–0.247 [112]		1.061 [32]	394.1–403.1 [116]
[Bmim][Ac]	293.0–348.0	0.001–0.207 [112]		1.053 [117]	391.6–402.1 [118]
H_2S absorbents					
[Bmim][BF_4]	303.1–343.1	15.5–33.4 [119]		1.204 [120]	363.1–368.7 [46]
[Bmim][PF_6]	303.1–343.1	18.6–33.8 [119]		1.370 [121]	407.7–413.1 [121]
[Bmim][NTf2]	303.1–343.1	13.7–26.6 [119]		1.436 [60]	567.3–572.8 [121]
[Hmim][BF_4]	303.1–343.1	12.5–25.7 [122]		1.145 [123]	427.8–433.0 [46]
[Hmim][PF_6]	303.1–343.1	17.9–39.7 [122]		1.294 [124]	469.0–476.0 [125]
[Hmim][NTf2]	303.1–343.1	17.4–40.6 [122]		1.371 [126]	631.6–632.9 [127]
[Emim][NTf2]	303.1–353.1	14.8–31.6 [128]		1.518 [25]	525.0–529.0 [106]
[Emim][$EtSO_4$]	303.1–353.1	60.7–133.0 [129]		1.237 [130]	394.4–399.3 [106]
[Omim][NTf2]	303.1–353.1	9.9–19.5 [123]		1.323 [132]	733.0–748.0 [106]
[Omim][PF_6]	303.1–353.1	12.2–25.5 [120]		1.235 [133]	536.0–544.0 [125]

lowest P_a within 299.15–323.15 K with values of 4.40–22.25 bar among the eight physical ILs that were analyzed for H_2S/CH_4 separation.

As illustrated in Figure 3, the absorption pressures of different CO_2 absorbents in physical absorbents are greater than those of chemical ILs/DES for CO_2 streams. For the same IL [Bmim][BF_4], the absorption pressures for different gas streams are as follows: effluent gases ($y_{CO_2} = 0.12$) > kiln gas $y_{CO_2} = 0.25$) > adipic acid off-gas ($y_{N_2O} = 0.45$) > biomass syngas ($y_{CO_2} = 0.3$) > biogas ($y_{CO_2} = 0.4$) > high-sulfur natural gas ($y_{H_2S} = 0.32$) > synthetic ammonia purge gas ($y_{NH_3} = 0.45$). The key factors influencing the absorption pressure are gas concentration and gas solubility in absorbents. The absorption pressures increase with increasing gas concentrations in the gas stream and decreasing gas solubilities. Meanwhile, the absorption pressure shows an increasing trend as gas solubility decreases. Due to the low solubility of N_2O in [Bmim][BF_4], adipic acid off-gas exhibits a higher absorption pressure than biomass syngas. However, due to the high concentration of H_2S, high-sulfur natural gas shows a lower absorption pressure than biogas.

4.1.2. Amount of Absorbent. Figures 5 and 6 show the absorbent amounts. As the desorption temperature rises, the amount of absorbents decreases, especially at low desorption temperatures.

The physical [Bmim][DCA] exhibits the lowest amount with values of 44.22–11.15 g·gCO_2^{-1}, 36.60–9.62 g·gCO_2^{-1}, and 32.26–6.84 g·gCO_2^{-1} within the range of 300.15–323.15 K for effluent gases, kiln gas, and biomass syngas, respectively, in the 30 physical absorbents. The chemical Ch[Pro]/PEG200 (1 : 2) represents the minimum values of m_{abs}, which are 13.39–5.62 g·gCO_2^{-1}, 14.60–4.63 g·gCO_2^{-1}, and 9.35–1.44 g·gCO_2^{-1} in 315.15–345.15 K, respectively. [P_{66614}][FAP] and [Omim][PF_6] exhibited the lowest amount with values of 104.59–6.71 g·gN_2O^{-1} and 4.72–14.74 g·gH_2S^{-1} for adipic acid off-gas and high-sulfur natural gas, respectively, within the range of 300.15–323.15 K.

Due to differences in CO_2 solubility, the amounts of CO_2 absorbents follow the order of chemical absorbents < -physical absorbents. Generally, the solubility of CO_2 in chemical absorbents is greater than that in physical absorbents. For different CO_2 streams with the same absorbents, the quantity has the following order: high-sulfur natural gas ($y_{H_2S} = 0.32$) > synthetic ammonia purge gas ($y_{NH_3} = 0.45$) > effluent gases ($y_{CO_2} = 0.12$) > kiln gas ($y_{CO_2} = 0.25$) > biomass syngas ($y_{H_2S} = 0.3$) > biogas ($y_{CO_2} = 0.4$) > adipic acid off-gas ($y_{H_2S} = 0.45$). The major reason for the significant amount of absorbents is the high gas solubility in high-sulfur natural gas and synthetic ammonia purge gas.

4.1.3. Energy Consumption. In Figures 7 and 8, the energy consumption is displayed. The energy consumption increases with an increase in the desorption temperature. The physical [Hmpy][NTf_2] displays the lowest Q_{tot} for the CO_2 separation process in the 30 physical absorbents, with values of 1.94–2.87 GJ·ton CO_2^{-1}, 1.02–1.49 GJ·ton CO_2^{-1} and 0.89–1.21 GJ·ton CO_2^{-1} for effluent gases, kiln gas, and biomass syngas, respectively, within the range of 299.15–323.15 K. The chemical [Eeim][Ac] exhibits the lowest energy consumption in the four chemical absorbents, with values of 2.48–3.70 GJ·ton CO_2^{-1}, 1.40–2.27 GJ·ton CO_2^{-1}, and 1.24–1.92 GJ·ton CO_2^{-1} respectively, within 303.15–345.15 K. The physical IL [Omim][PF_6] exhibits the lowest energy consumption for the separation of H_2S from high-sulfur natural gas in the 10 physical ILs, with values of 1.05–1.44 GJ·ton H_2S^{-1} within 299.15–323.15 K for high-sulfur natural gas. [P_{66614}][FAP] shows the lowest energy consumption for N_2O separation in the 8 physical ILs, with values of 0.65–0.95 GJ·ton H_2S^{-1} within 299.15–323.15 K for adipic acid off-gas.

Due to the high heat of chemical absorbents, the energy consumption of chemical absorbents is larger than that of physical absorbents. The CO_2 concentrations have an impact on the energy consumption for various CO_2 streams. The energy consumption sequence is as follows: effluent gases ($y_{CO_2} = 0.12$) > synthetic ammonia purge gas ($y_{NH_3} = 0.45$) > kiln gas ($y_{CO_2} = 0.25$) > biomass syngas ($y_{CO_2} = 0.3$) > high-sulfur natural gas ($y_{H_2S} = 0.32$) > biogas ($y_{CO_2} = 0.4$) > adipic acid off-gas ($y_{N_2O} = 0.45$). The energy consumption for separating CO_2 from effluent gases (CO_2/N_2) is the largest due to the low CO_2 molar ratio, and the energy consumption for separating N_2O from adipic acid off-gas is the lowest due to the highest N_2O solubility and a high amount of absorbents.

4.2. Screening Absorbents. The screening criteria for absorbents include both absorbent amounts (m_{abs}) and energy consumption (Q_{tot}). The physical [Bmim][DCA] was screened between 299.15–323.15 K with low amounts of the absorbent (<190 g·gCO_2^{-1} for effluent gases, <150 g·gCO_2^{-1} for kiln gas, <140 g·gCO_2^{-1} for biomass syngas) and low energy consumption (<2 GJ·tonCO_2^{-1} for effluent gases, <1 GJ·tonCO_2^{-1} for kiln gas, <0.9 GJ·tonCO_2^{-1} for biomass syngas). The chemical [Eeim][Ac] was screened with a lower amount of ILs (<43 g·gCO_2^{-1} for effluent gases at 303.15–345.15 K, <142 g·gCO_2^{-1} for kiln gas at 299.15–345.15 K, <68 g·gCO_2^{-1} for biomass syngas at 300.15–345.15 K). A lower amount of ILs (<293 g·gH_2S^{-1}) was used to screen [Omim][PF_6] for high-sulfur natural gas at 299.15–323.15 K. A lower amounts of ILs (<108 g·gN_2O^{-1}) was used to screen [P_{66614}][FAP] for adipic acid off-gas at 299.15–323.15 K. The uncertainties of Henry's law constant, heat capacity, and density were taken into consideration while estimating the uncertainties in the iterated results. The uncertainties in the absorption pressure, the required amount of ILs, and the energy expended for CO_2 separation were estimated to be ±3.97 bar, ±2.47 g·gCO_2^{-1}, and ±0.09 GJ·tonCO_2^{-1}, respectively. The uncertainties in the absorption pressure, the required amount of ILs, and the energy expended for H_2S separation were estimated to be ±0.41 bar, ±0.37 g·gH_2S^{-1}, and ±0.003 GJ·tonH_2S^{-1}, respectively. The uncertainties in the absorption pressure, the required amount of ILs, and the energy used for N_2O separation were estimated to be ±0.12 bar, ±0.17 g·gN_2O^{-1},

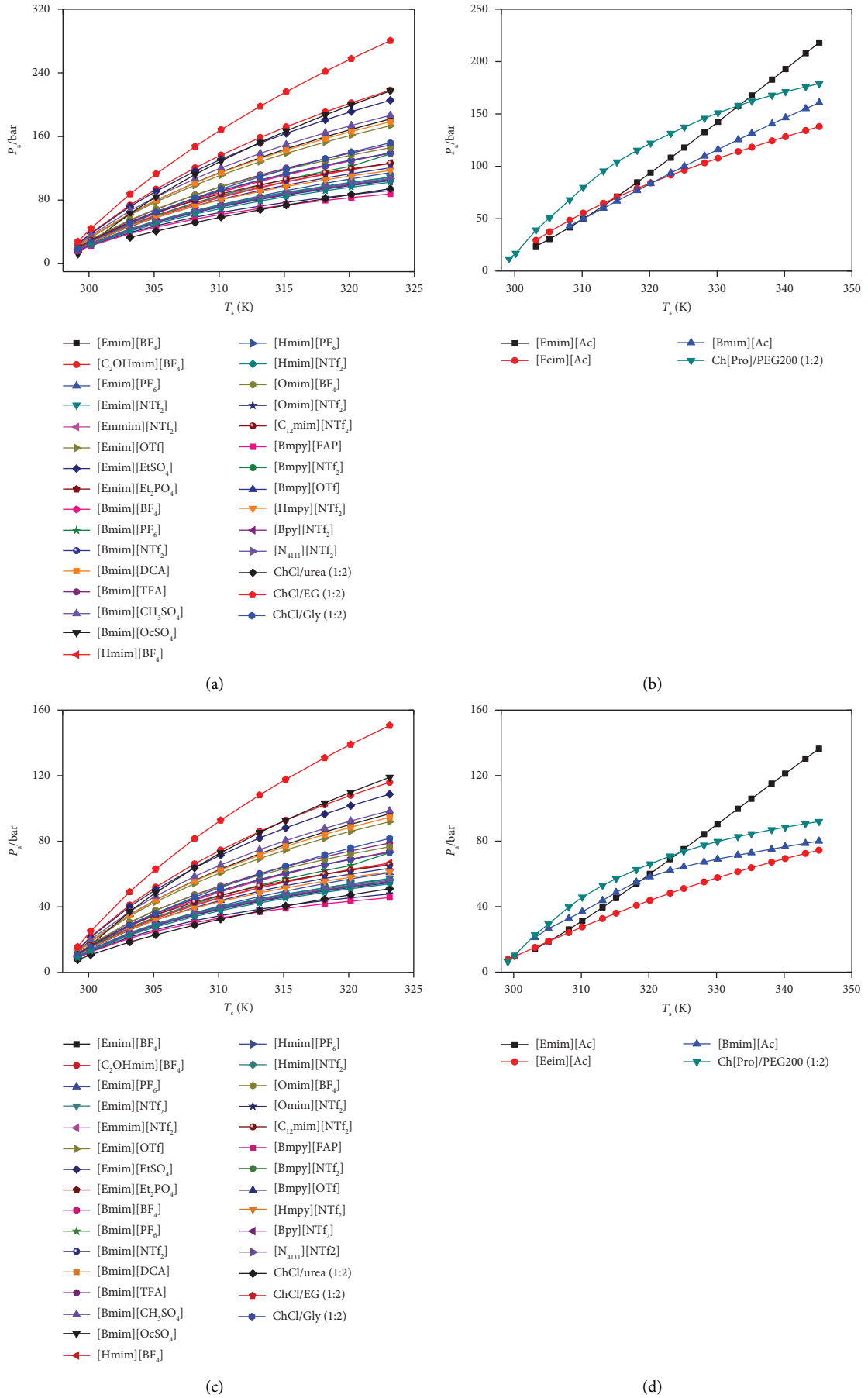

Figure 3: Continued.

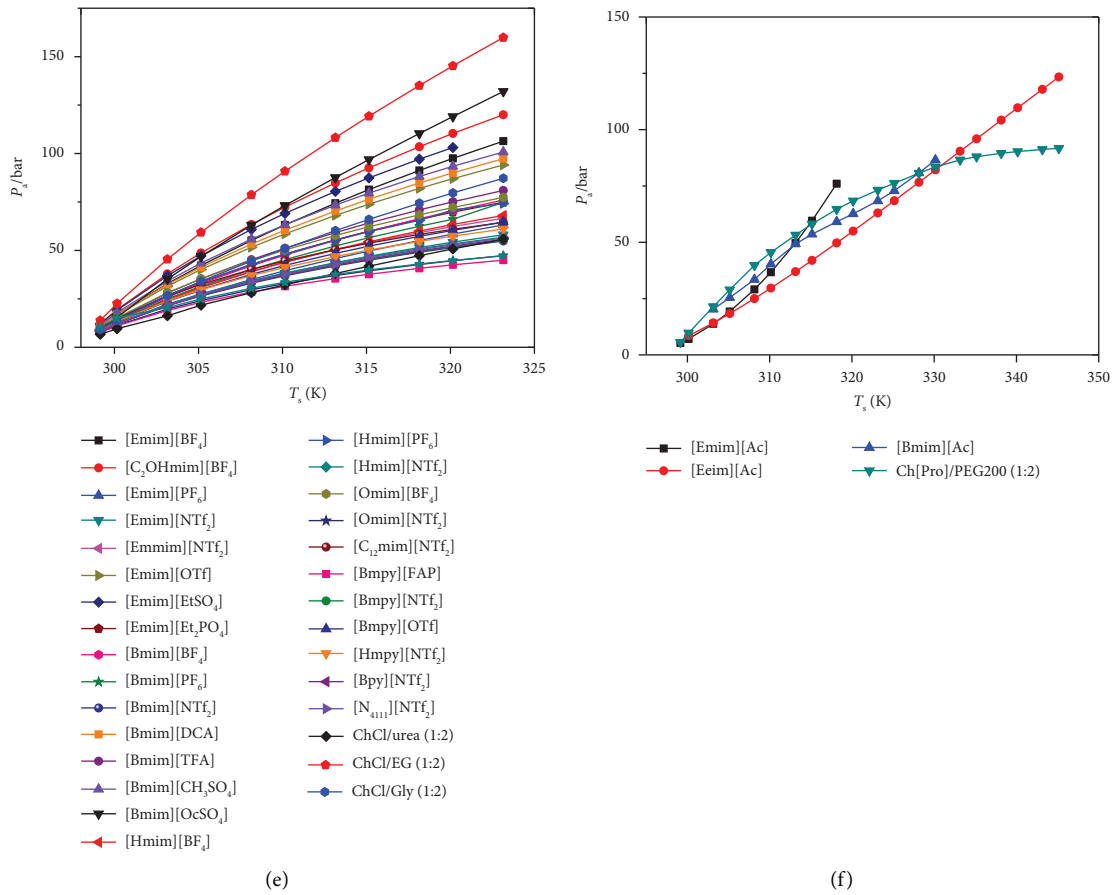

(e) (f)

Figure 3: The absorption pressures of (a) 30 physical absorbents for effluent gases, (b) 4 chemical absorbents for effluent gases, (c) 30 physical absorbents for kiln gas, (d) 4 chemical absorbents for kiln gas, (e) 30 physical absorbents for biomass syngas, and (f) 4 chemical absorbents for biomass syngas.

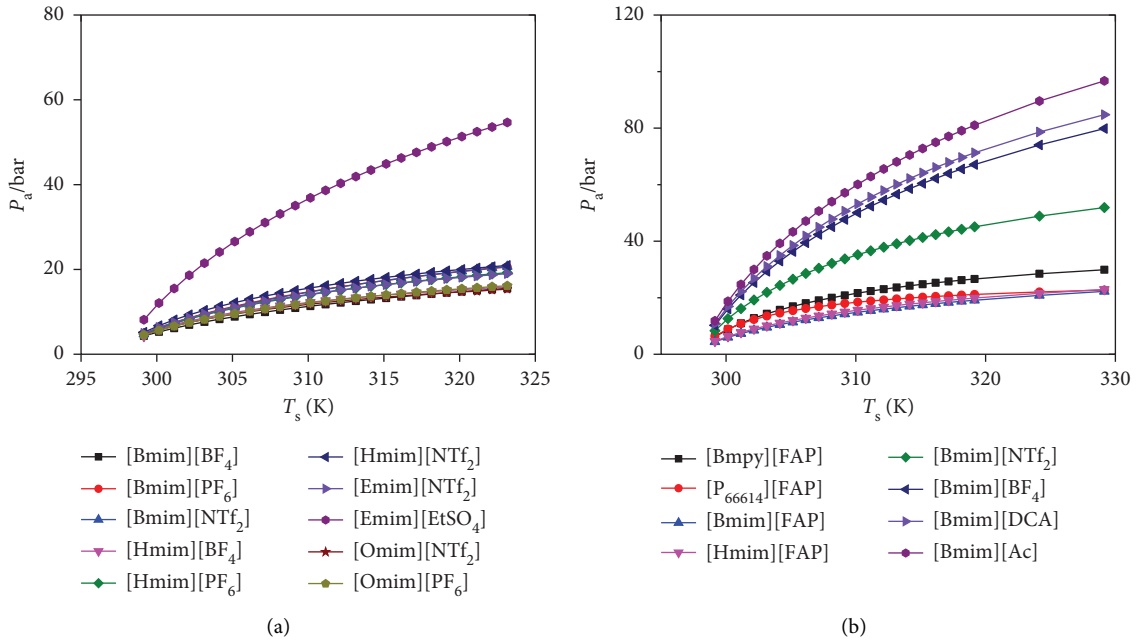

(a) (b)

Figure 4: The absorption pressures of (a) 10 physical absorbents for high-sulfur natural gas and (b) 8 physical absorbents for adipic acid off-gas.

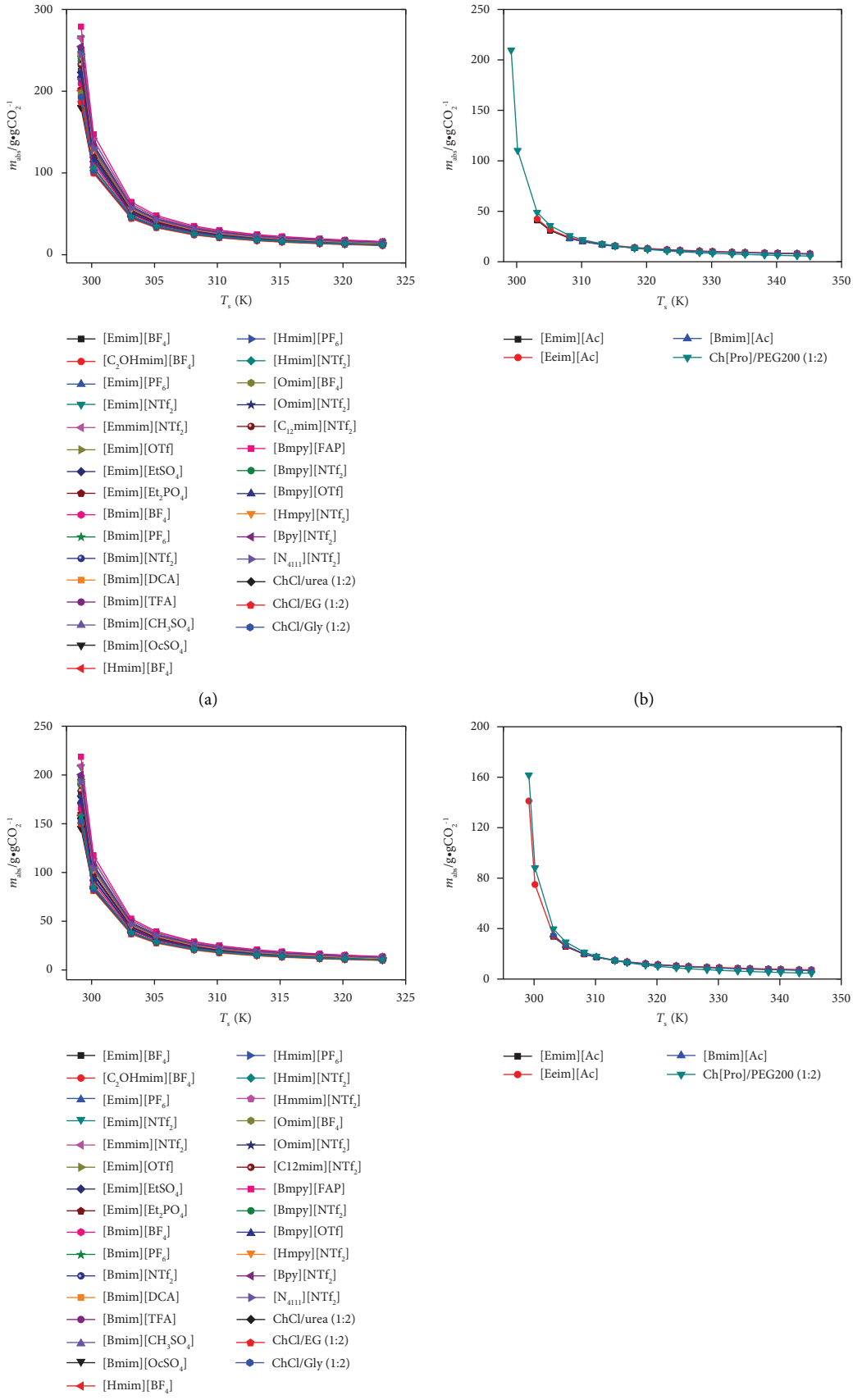

Figure 5: Continued.

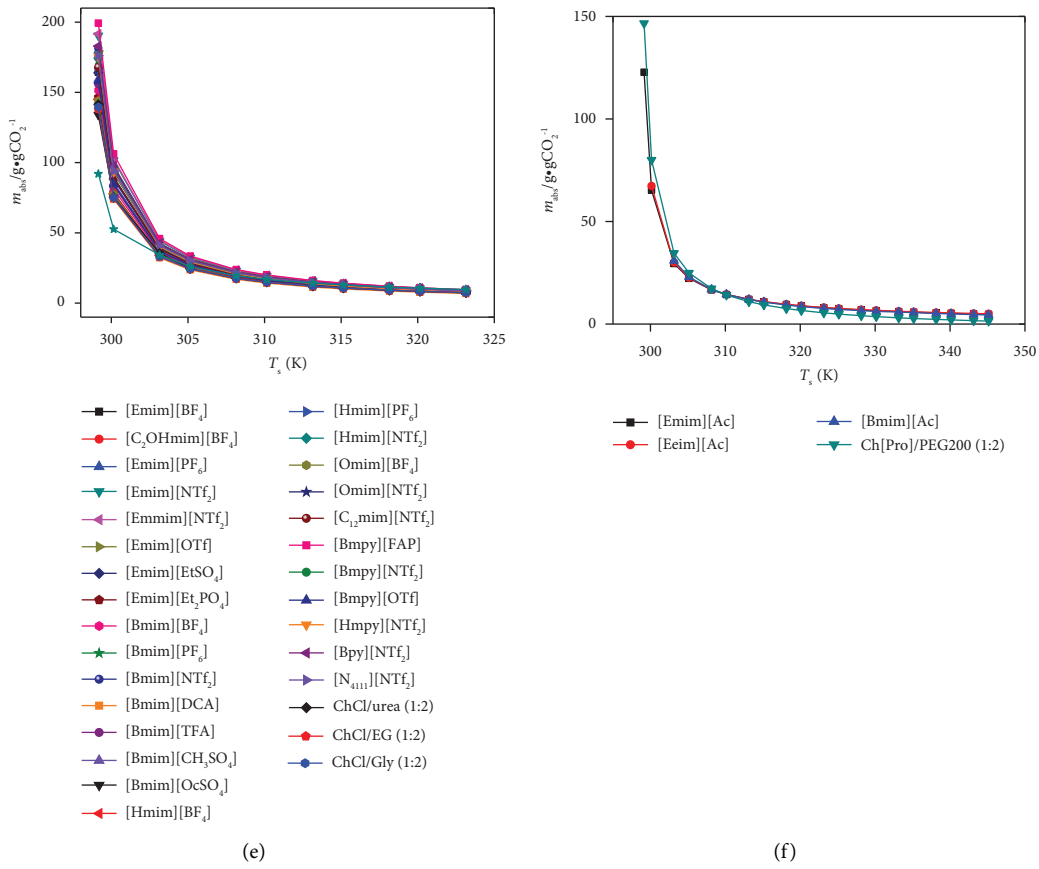

Figure 5: The absorbent amount of (a) 30 physical absorbents for effluent gases, (b) 4 chemical absorbents for effluent gases, (c) 30 physical absorbents for kiln gas, (d) 4 chemical absorbents for kiln gas, (e) 30 physical absorbents for biomass syngas, and (f) 4 chemical absorbents for biomass syngas.

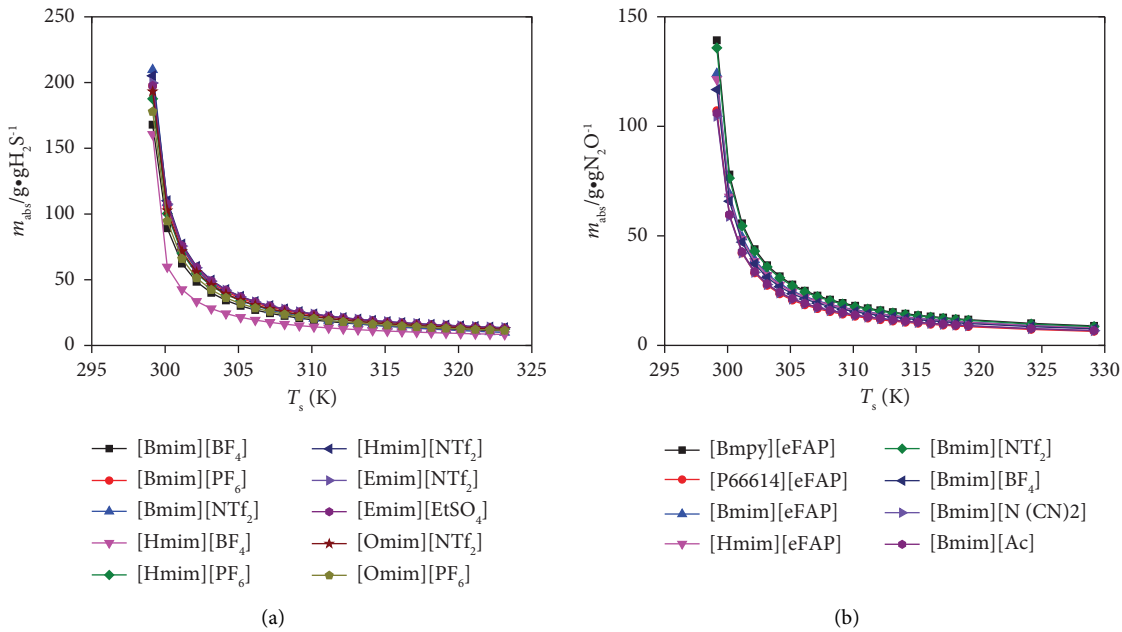

Figure 6: The absorbent amount of (a) 10 physical absorbents for high-sulfur natural gas and (b) 8 physical absorbents for adipic acid off-gas.

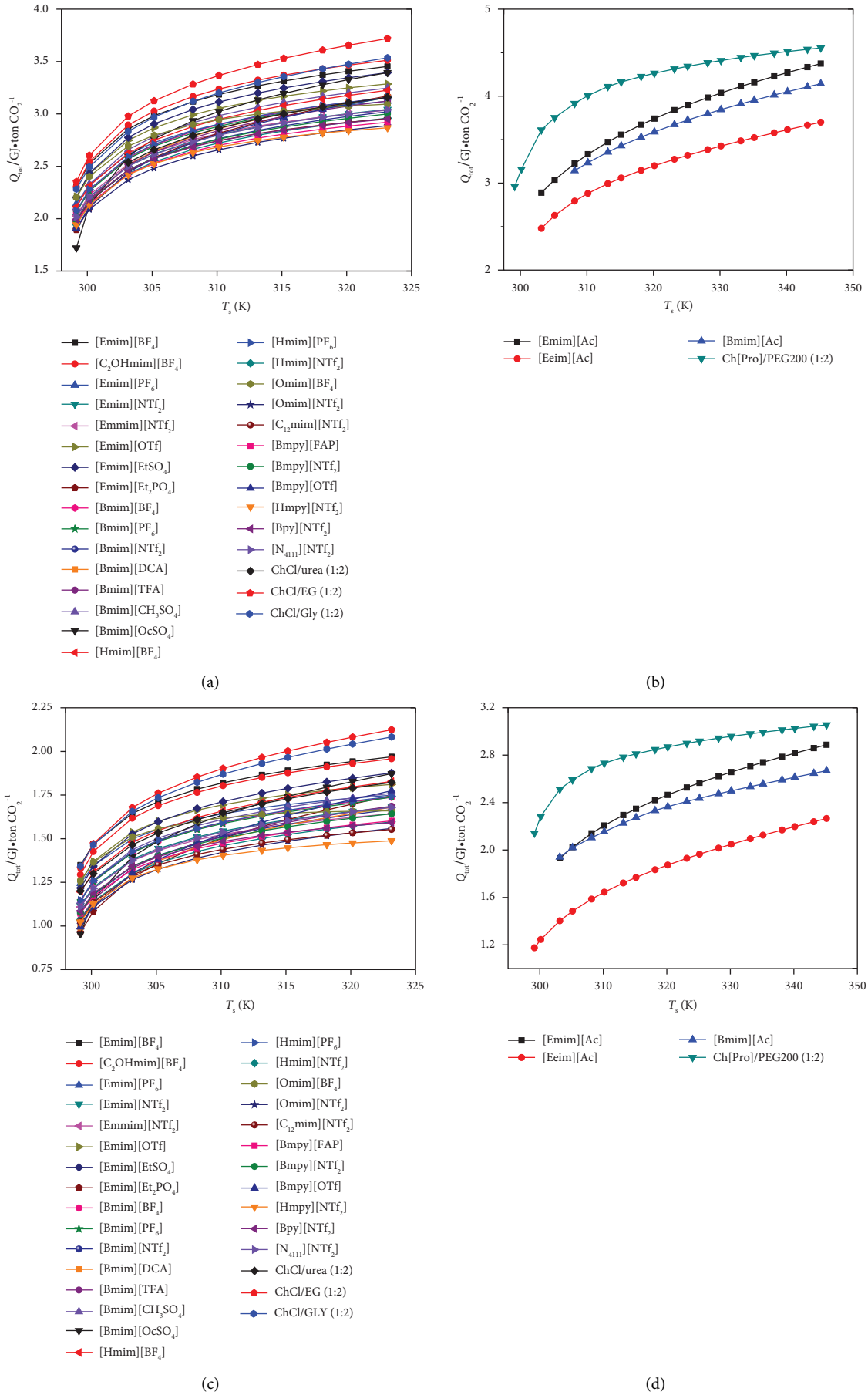

Figure 7: Continued.

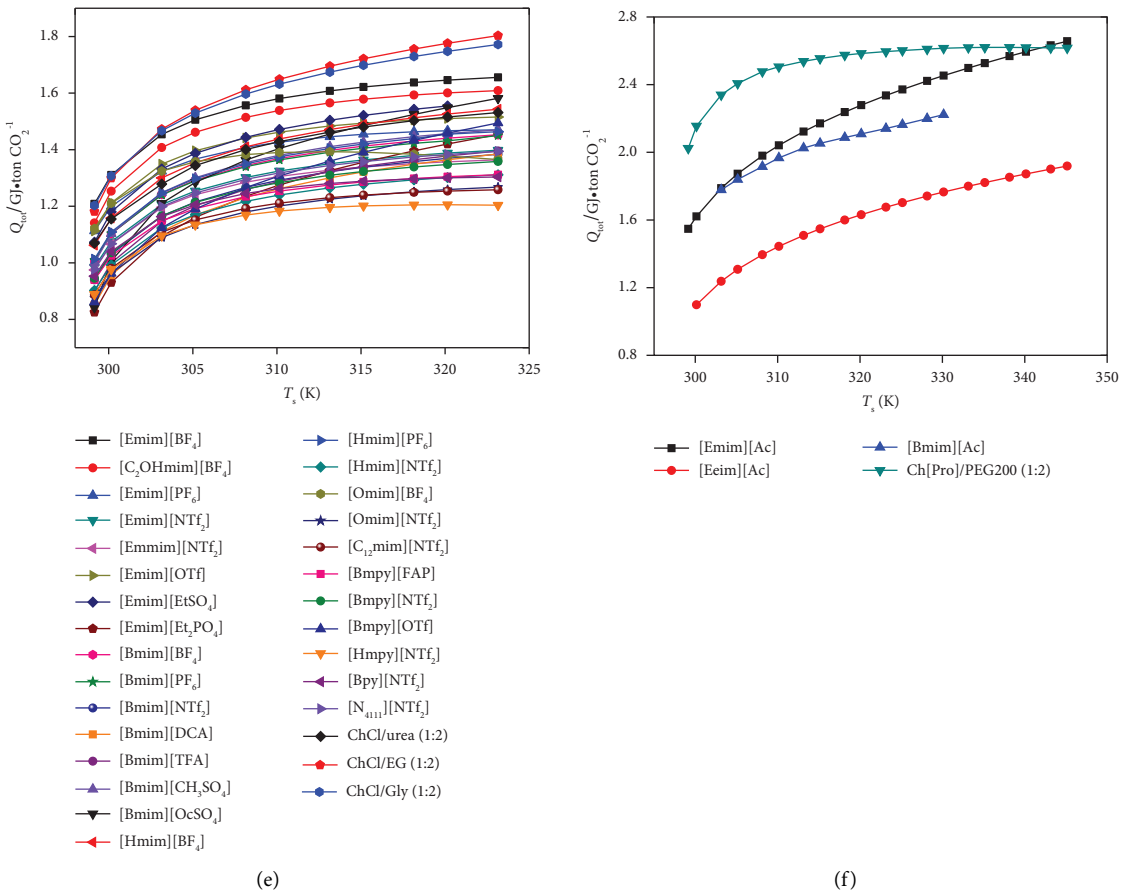

Figure 7: The energy consumption of (a) 30 physical absorbents for effluent gases, (b) 4 chemical absorbents for effluent gases, (c) 30 physical absorbents for kiln gas, (d) 4 chemical absorbents for kiln gas, (e) 30 physical absorbents for biomass syngas, and (f) 4 chemical absorbents for biomass syngas.

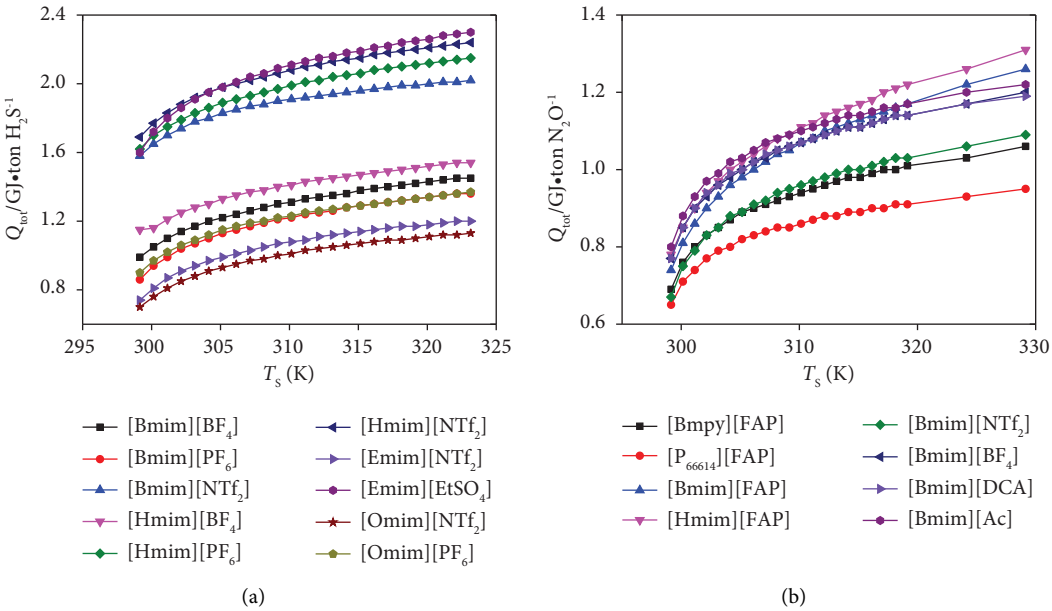

Figure 8: The energy consumption of (a) 10 physical absorbents for high-sulfur natural gas and (b) 8 physical absorbents for adipic acid off-gas.

Table 3: The optimal condition (T_s, P_a), the absorbents amounts (m_{abs}), and the energy consumption (Q_{tot}) of the screened absorbents.

Absorbents	CO_2 streams	T_s (K)	P_a (bar)	m_{abs} (g•gX^{-1})	Q_{tot} (GJ•tonX^{-1})
[Bmim][DCA]	Effluent gases	299.15–323.15	22.21–178.58	188.41–12.37	1.95–3.16
	Kiln gas	299.15–323.15	12.33–94.60	150.01–10.63	0.99–1.68
	Biomass syngas	299.15–323.15	10.88–97.35	137.70–7.80	0.85–1.39
	Biogas [11]	299.15–323.15	8.75–64.34	124.21–8.64	0.73–1.04
[Eeim][Ac]	Effluent gases	303.15–345.15	29.43–137.96	42.31–8.10	2.48–3.70
	Kiln gas	299.15–345.15	7.81–74.44	141.14–7.33	1.18–2.27
	Biomass syngas	300.15–345.15	8.46–123.37	67.36–5.01	1.10–1.92
	Biogas [11]	299.15–345.15	4.30–59.99	108.11–6.93	0.84–1.82
[Omim][PF_6]	High-sulfur natural gas	299.15–323.15	3.97–14.74	290.77–14.72	1.05–1.44
[P_{66614}][FAP]	Adipic acid off-gas	299.15–323.15	6.40–22.71	107.13–6.42	0.65–0.95
[Omim][BF_4]	Synthetic ammonia purge [13]	299.15–319.15	3.31–11.06	20.12–257.05	1.05–1.91

Table 4: The optimal conditions (T_s, P_a), the absorbent amounts (m_{abs}), and the energy consumption (Q_{tot}) of the commercial absorbents.

Absorbents	Gas streams	T_s (K)	P_a (bar)	m_{abs} (g•gX^{-1})	Q_{tot} (GJ•tonX^{-1})
30 wt % MEA	Effluent gases	373.15–393.15	75.18–105.16	2.31–1.97	5.29–5.57
	Kiln gas	373.15–393.15	102.66–144.38	2.20–1.89	3.88–4.05
	Biomass syngas	373.15–393.15	65.20–114.38	2.36–1.95	3.28–3.37
	Biogas [11]	373.15–393.15	6.50–23.73	3.51–2.43	3.80–3.84
30 wt % MDEA	Effluent gases	373.15–393.15	39.10–53.78	2.34–2.02	3.79–4.10
	Kiln gas	373.15–393.15	54.12–74.71	2.23–1.94	2.94–3.17
	Biomass syngas	373.15–393.15	45.56–80.19	2.29–1.92	2.77–3.01
	Biogas [11]	373.15–393.15	0.96–2.64	5.70–3.66	2.66–2.50
DEPG for selexol	Effluent gases	299.15–323.15	16.68–102.43	200.57–12.29	1.75–2.55
	Kiln gas	299.15–323.15	9.08–54.03	157.58–10.54	0.92–1.28
	Biomass syngas	299.15–323.15	7.97–55.07	143.82–7.36	0.82–1.13
	Biogas [11]	299.15–323.15	6.38–36.11	128.45–9.40	0.69–0.88
H_2O	High-sulfur natural gas	299.15–323.15	11.77–119.58	102.88–7.14	0.77–1.56

and ± 0.04 GJ·tonN_2O^{-1}, respectively. Table 3 lists the screened absorbents and their values of T_s, P_a, m_{abs}, and Q_{tot}.

4.3. Comparison with Commercial Absorbents. The superiority of the screened absorbents is demonstrated by comparisons with commercial absorbents. For CO_2 separation, the chemical [Eeim][Ac] in this study is compared with 30% MEA and 30% MDEA. [Bmim][DCA] is compared with DEPG for CO_2 separation. Furthermore, for H_2S separation, [Omim][PF_6] is compared with water. The findings of P_a, m_{abs}, and Q_{tot} of commercial absorbents for gas separation from effluent gases, kiln gas and biomass syngas, biogas, high-sulfur natural gas, and adipic acid off-gas are displayed in Table 4 with the set desorption temperature.

The results of m_{abs} and Q_{tot} for [Bmim][DCA] and DEPG are displayed in Figures 9 and 10. Figure 11 displays the predicted results of m_{abs} and Q_{tot} for chemical [Eeim][Ac] at 338.15 K, 30 wt% MEA at 393.15 K, and 30 wt% MDEA at 393.15 K.

Based on the comparisons of the performances of physical absorbents for CO_2 separation shown in Figures 9 and 10, both energy consumption and the amount required for DEPG are lower than those of [Bmim][DCA] when P_a is 12.5 bar and 25 bar, respectively. This suggests that the performance of the screened ILs is not superior to that of commercial physical absorbents for DEPG. Based on the comparison of the performances of chemical absorbents for CO_2 streams in Figure 11, [Eeim][Ac] displays a larger absorbent amount and lower energy consumption than those of 30 wt% MDEA and 30 wt% MEA. Assuming that the cost of [Eeim][Ac] is high, the screening of chemical ILs for CO_2 separation must be further researched. However, the volatility of [Eeim][Ac] can be ignored.

From the comparison of the performances of physical absorbents for the H_2S stream in Figure 12, [Omim][BF_4] exhibited higher energy consumption and a lower amount of absorbents. The comparison of [Omim][BF_4] and DEPG shows that the performance of physical IL is not superior to that of DEPG. The screened ILs have the advantage of low energy consumption and nonvolatility, although they have a higher amount than chemical CO_2 absorbents (30 wt% MDEA and 30 wt% MEA). The physical H_2S absorbent consumes less energy than water.

The cost of conventional ILs is significantly higher than that of commercial CO_2 absorbents when operational costs and solvent costs are considered. For instance, the estimated costs of water, DEPG, MEA, and MDEA were estimated to be 0.3×10^{-3} US$·kg^{-1} [134], 3.5 US$·kg^{-1} [135],

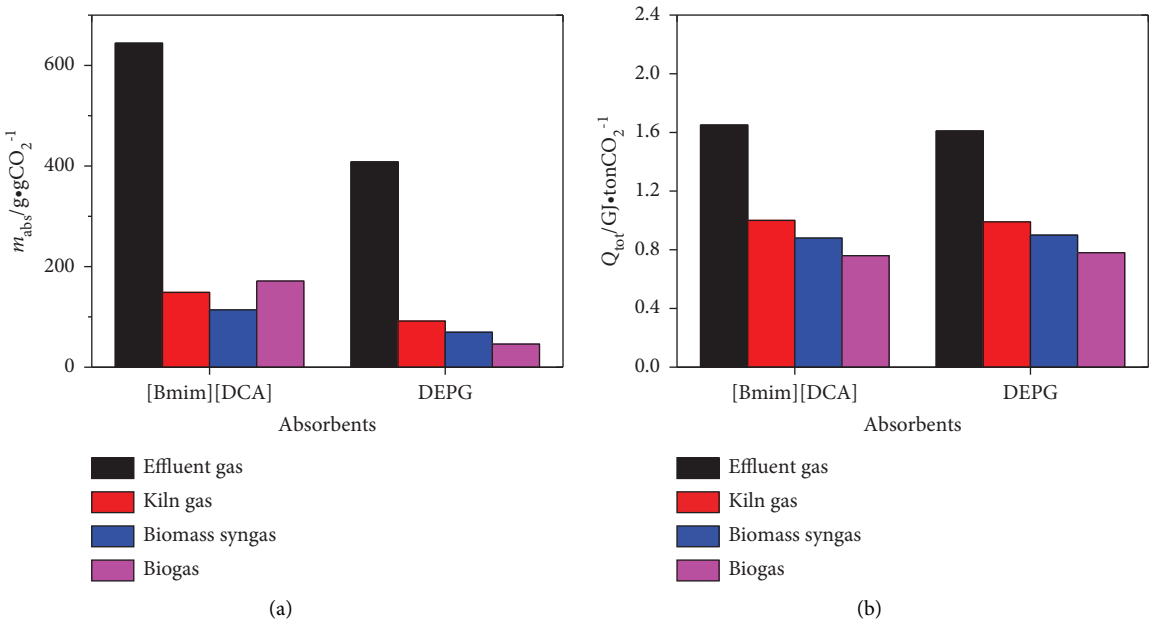

Figure 9: The comparison of the performances of physical absorbents with P_a at 12.5 bar for CO_2 streams.

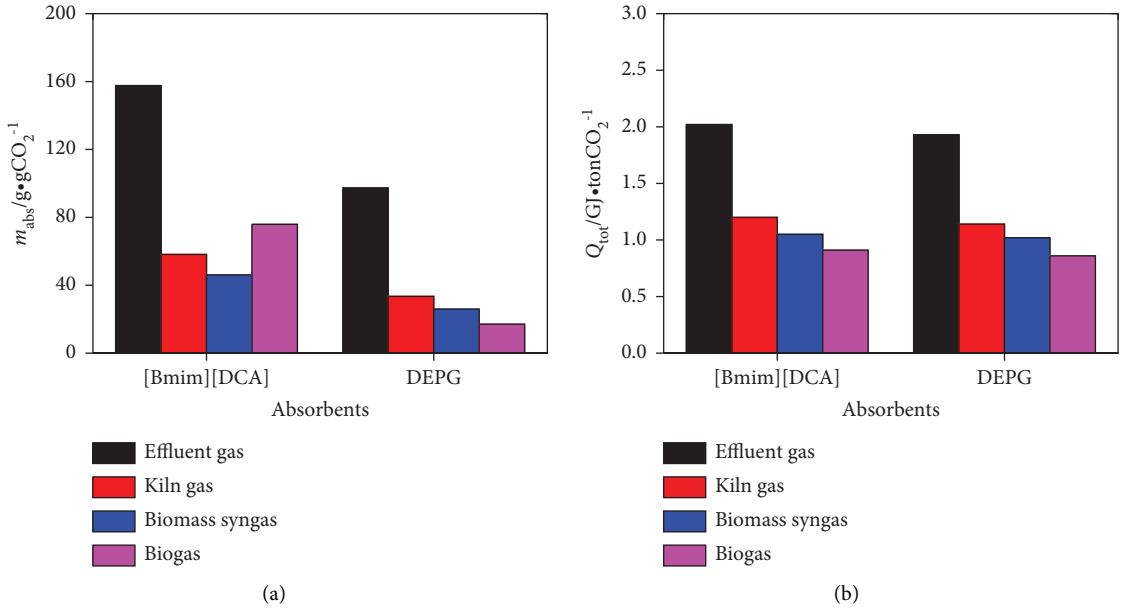

Figure 10: The comparison of the performances of physical absorbents with P_a at 25 bar for CO_2 streams.

1.25–2.25 US$·kg^{-1} [136, 137], and 20 US$·kg^{-1} [138], respectively, while the cost of the used commercial ILs was estimated as 6–13.5 US$·kg^{-1} [136]. Both the price and the amount needed of conventional ILs are higher than those of commercial gas absorbents; therefore, the advantages of ILs are located at nonvolatility, low energy use for chemical absorbents, and nondegradability. It is needed to develop process simulation with consideration of solvent degradation to compare conventional ILs and commercial gas absorbents. Furthermore, with technological advancement, the cost of ILs will drop, and the cost difference between conventional ILs and commercial absorbents will reduce.

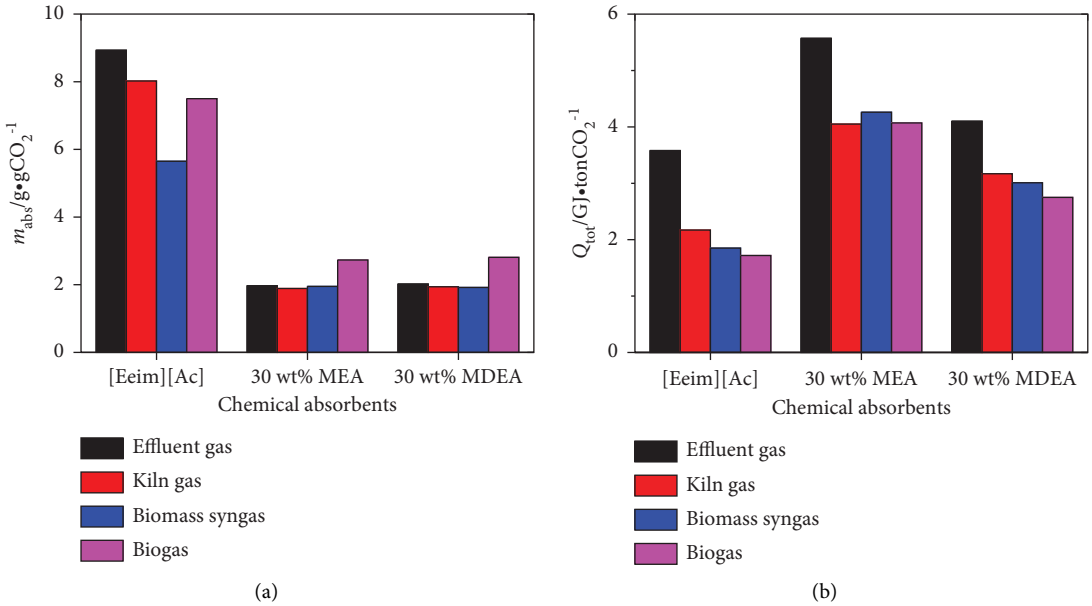

Figure 11: The comparison of the performances of chemical absorbents for CO_2 streams.

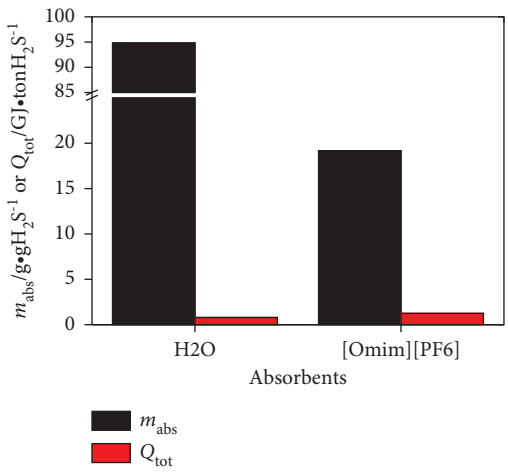

Figure 12: The comparison of the performances of physical absorbents for the H_2S stream.

5. Conclusions

In this study, green absorbents were analyzed based on ΔG to screen the absorbents for CO_2 separation from effluent gases, kiln gas, and biomass syngas; H_2S separation from high-sulfur natural gas (H_2S/CH_4); and N_2O separation from adipic acid off-gas (N_2O/N_2).

[Bmim][DCA] and [Eeim][Ac] were screened for CO_2 separation using m_{abs} and Q_{tot} as criteria. [Omim][PF_6] and [P_{66614}][FAP] were screened for H_2S separation and N_2O separation, respectively. According to comparisons between the screened absorbents and the DEPG, the physical IL has a higher energy consumption and higher m_{abs} than the DEPG. When compared with 30 wt% MDEA and 30 wt% MEA, the chemical IL has a lower Q_{tot} and is involatile. Lower energy consumption and a higher amount of H_2S separation were observed when screened [Omim][BF_4] was compared to H_2O.

Due to the differences in gas concentration in gas streams and gas solubility in absorbents, the amount of absorbents has the following order: high-sulfur natural gas > synthetic ammonia purge gas > effluent gases > kiln gas > biomass syngas > biogas > adipic acid off-gas. The order of energy consumption is as follows: effluent gases > synthetic ammonia purge gas > kiln gas > biomass syngas > high-sulfur natural gas > biogas > adipic acid off-gas.

Data Availability

The data used to support the findings of this study are from previously reported studies and datasets, which are cited in the article. The enthalpy and entropy of gas components are available and can be found at NIST Standard Reference Data (https://webbook.nist.gov/chemistry/fluid/).

Conflicts of Interest

The authors declare that they have no conflicts of interest.

Acknowledgments

This work was supported by the Scientific and Technological Key Project in Henan Province (grant no. 22A530004), Ph.D. Research Startup Foundation of the Zhengzhou University of Light Industry (grant nos. 2017BSJJ029 and 2020BSJJ018), and the National College Students' Innovation and Entrepreneurship Training Program (grant no. 202210462074).

Supplementary Materials

Appendix A: supplementary data associated with this article. (*Supplementary Materials*)

References

[1] United States Environmental Protection Agency, *Inventory of U.S. Greenhouse Gas Emissions and Sinks: 1990-2018*, United States Environmental Protection Agency, Washington DC, USA, 2020.

[2] O. Edenhofer, *Climate Change 2014 Mitigation of Climate Change*, Cambridge University, Cambridge, UK, 2014.

[3] M. K. Mondal, H. K. Balsora, and P. Varshney, "Progress and trends in CO_2 capture/separation technologies: a review," *Energy*, vol. 46, no. 1, pp. 431–441, 2012.

[4] V. Ramanathan, "Trace-gas greenhouse effect and global warming: underlying principles and outstanding issues - volvo Environmental Prize lecture 1997," *Ambio*, vol. 27, pp. 187–197, 1998.

[5] X. H. Liu, "Discussion on new methods of hydrogen sulfide waste gas treatment," *Science & Technology Information*, vol. 17, no. 31, pp. 61–63, 2019.

[6] A. L. Kohl and R. B. Nielsen, "Mechanical Design and Operation of Alkanolamine Plants," *Gas Purification*, pp. 187–277, Gulf Professional Publishing, Houston, Texas, Fifth edition, 1997.

[7] E. L. Smith, A. P. Abbott, and K. S. Ryder, "Deep eutectic solvents (DESs) and their applications," *Chemical Reviews*, vol. 114, no. 21, pp. 11060–11082, 2014.

[8] Q. H. Zhang, K. De Oliveira Vigier, S. Royer, and F. Jerome, "Deep eutectic solvents: syntheses, properties and applications," *Chemical Society Reviews*, vol. 41, no. 21, pp. 7108–7146, 2012.

[9] G. Garcia, S. Aparicio, R. Ullah, and M. Atilhan, "Deep eutectic solvents: physicochemical properties and gas separation applications," *Energy and Fuels*, vol. 29, no. 4, pp. 2616–2644, 2015.

[10] Z. P. Cai, J. Y. Zhang, Y. D. Ma et al., "Chelation-activated multiple-site reversible chemical absorption of ammonia in ionic liquids," *American institute of chemical engineers Journal*, vol. 68, no. 5, Article ID e17632, 2022.

[11] S. Sarmad, J. P. Mikkola, and X. Y. Ji, "Carbon dioxide capture with ionic liquids and deep eutectic solvents: a new generation of sorbents," *ChemSusChem*, vol. 10, no. 2, pp. 324–352, 2017.

[12] N. N. Cheng, Z. L. Li, H. C. Lan, W. L. Xu, and K. Huang, "Remarkable NH_3 absorption in metal-based deep eutectic solvents by multiple coordination and hydrogen-bond interaction," *American institute of chemical engineers Journal*, vol. 68, no. 6, Article ID 17660, 2022.

[13] Y. N. Cao, J. Y. Zhang, Y. D. Ma, W. Q. Wu, K. Huang, and L. L. Jiang, "Designing low-viscosity deep eutectic solvents with multiple weak-acidic groups for ammonia separation," *ACS Sustainable Chemistry & Engineering*, vol. 9, no. 21, pp. 7352–7360, 2021.

[14] C. T. Li, Z. P. Cai, Y. D. Ma, Y. N. Cao, K. Huang, and L. L. Jiang, "Densities and viscosities of, and solubilities of acidic gases (SO_2 and H_2S) in natural deep eutectic solvents [J]," *The Journal of Chemical Thermodynamics*, vol. 167, Article ID 106713, 2022.

[15] Y. Y. Zhang, X. Y. Ji, Y. J. Xie, and X. H. Lu, "Thermodynamic analysis of CO_2 separation from biogas with conventional ionic liquids," *Applied Energy*, vol. 217, pp. 75–87, 2018.

[16] Y. Y. Zhang, X. Y. Ji, and X. H. Lu, "Choline-based deep eutectic solvents for CO_2 separation: review and thermodynamic analysis," *Renewable and Sustainable Energy Reviews*, vol. 97, pp. 436–455, 2018.

[17] Y. Y. Zhang, S. N. Guo, S. L. Song et al., "Thermodynamic analysis for NH_3 separation using ionic liquids/deep eutectic solvents," *Computers and industrial engineering Journal*, vol. 72, no. 3, pp. 1264–1274, 2021.

[18] Y. P. Li, T. J. Wang, X. L. Yin et al., "Design and operation of integrated pilot-scale dimethyl ether synthesis system via pyrolysis/gasification of corncob," *Fuel*, vol. 88, no. 11, pp. 2181–2187, 2009.

[19] D. G. Chapel, C. L. Mariz, and J. Ernest, "Recovery of CO2 from Flue Gases: Commercial Trends," *Canadian Society of Chemical Engineers annual meeting*, citeseer, Princeton, NJ, USA, 1999.

[20] P. Lundqvist, *Mass and Energy Balances over the Lime kiln in a Kraft Pulp Mill*, Uppsala University, Uppsala, Sweden, 2009.

[21] A. Bes, "Dynamic Process Simulation of limestone Calcination in normal Shaft Kilns," 2006, https://opendata.uni-halle.de/bitstream/1981185920/10758/1/agnbes.pdf.

[22] B. Y.. Wo, "63 well with high sulfur content was successfully opened," *Natural Gas Industry*, vol. 14, no. 2, p. 25, 1994.

[23] H. S. Cheng, *Applied Abatement Technology of N_2O in Adipic Acid Production in Liaoyang Petrochemical Company*, Tsinghua Unviersity, Beijing, China, 2010.

[24] A. N. Soriano, B. T. Doma, and M. H. Li, "Solubility of carbon dioxide in 1-ethyl-3-methylimidazolium tetrafluoroborate," *Journal of Chemical & Engineering Data*, vol. 53, no. 11, pp. 2550–2555, 2008.

[25] S. Seki, S. Tsuzuki, K. Hayamizu et al., "Comprehensive refractive index property for room-temperature ionic liquids," *Journal of Chemical & Engineering Data*, vol. 57, no. 8, pp. 2211–2216, 2012.

[26] Y. A. Sanmamed, D. González-Salgado, J. Troncoso, L. Romani, A. Baylaucq, and C. Boned, "Experimental methodology for precise determination of density of RTILs as a function of temperature and pressure using vibrating tube densimeters," *The Journal of Chemical Thermodynamics*, vol. 42, no. 4, pp. 553–563, 2010.

[27] C. M. S. S. Neves, K. A. Kurnia, J. A. P. Coutinho et al., "Systematic study of the thermophysical properties of imidazolium-based ionic liquids with cyano-functionalized anions," *The Journal of Physical Chemistry B*, vol. 117, no. 35, pp. 10271–10283, 2013.

[28] D. Waliszewski, I. Stępniak, H. Piekarski, and A. Lewandowski, "Heat capacities of ionic liquids and their heats of solution in molecular liquids," *Thermochimica Acta*, vol. 433, no. 1-2, pp. 149–152, 2005.

[29] Y. A. Sanmamed, P. Navia, D. González-Salgado, J. Troncoso, and L. Romaní, "Pressure and temperature dependence of isobaric heat capacity for [Emim] [BF_4], [Bmim] [BF_4], [Hmim] [BF_4], and [Omim] [BF_4]," *Journal of Chemical & Engineering Data*, vol. 55, no. 2, pp. 600–604, 2010.

[30] V. K. Sharma, S. Bhagour, S. Solanki, and A. Rohilla, "Thermodynamic properties of ternary mixtures containing ionic liquids and organic solvents," *Journal of Chemical & Engineering Data*, vol. 58, no. 7, pp. 1939–1954, 2013.

[31] Y.-H. Yu, A. N. Soriano, and M.-H. Li, "Heat capacity and electrical conductivity of aqueous mixtures of [Bmim] [BF_4] and [Bmim] [PF_6] [J]," *Journal of the Taiwan Institute of Chemical Engineers*, vol. 40, no. 2, pp. 205–212, 2009.

[32] M. Shokouhi, M. Adibi, A. H. Jalili, M. Hosseini Jenab, and A. Mehdizadeh, "Solubility and diffusion of H_2S and CO_2 in the ionic liquid 1-(2-hydroxyethyl)-3-methylimidazolium

tetrafluoroborate," *Journal of Chemical & Engineering Data*, vol. 55, no. 4, pp. 1663–1668, 2010.

[33] D. Song and J. Chen, "Densities and viscosities for ionic liquids mixtures containing [eOHmim] [BF_4], [bmim] [BF_4] and [bpy] [BF_4] [J]," *The Journal of Chemical Thermodynamics*, vol. 77, pp. 137–143, 2014.

[34] L. C. Branco, J. N. Rosa, J. J. Moura Ramos, and C. A. M. Afonso, "Preparation and characterization of new room temperature ionic liquids," *Chemistry--A European Journal*, vol. 8, no. 16, pp. 3671–3677, 2002.

[35] R. Taguchi, H. Machida, Y. Sato, and R. L. Smith, "High-pressure densities of 1-alkyl-3-methylimidazolium hexafluorophosphates and 1-alkyl-3-methylimidazolium tetrafluoroborates at temperatures from (313 to 473) K and at pressures up to 200 MPa," *Journal of Chemical & Engineering Data*, vol. 54, no. 1, pp. 22–27, 2009.

[36] P. B. P. Serra, *Thermal Behaviour and Heat Capacity of Ionic Liquids: Benzilimidazolium and Alkylimidazolium Derivatives*, Universidade do Porto, Porto, Portugal, 2013.

[37] C. Cadena, J. L. Anthony, J. K. Shah, T. I. Morrow, J. F. Brennecke, and E. J. Maginn, "Why is CO_2 so soluble in imidazolium-based ionic liquids?" *Journal of the American Chemical Society*, vol. 126, no. 16, pp. 5300–5308, 2004.

[38] D. Camper, C. Becker, C. Koval, and R. Noble, "Low pressure hydrocarbon solubility in room temperature ionic liquids containing imidazolium rings interpreted using regular solution theory," *Industrial & Engineering Chemistry Research*, vol. 44, no. 6, pp. 1928–1933, 2005.

[39] J. Jacquemin, P. Husson, V. Majer, and M. F. Costa Gomes, "Influence of the cation on the solubility of CO_2 and H_2 in ionic liquids based on the bis(trifluoromethylsulfonyl)imide anion," *Journal of Solution Chemistry*, vol. 36, no. 8, pp. 967–979, 2007.

[40] M. Součková, J. Klomfar, and J. Pátek, "Measurements and group contribution analysis of 0.1MPa densities for still poorly studied ionic liquids with the [PF_6] and [NTf_2] anions," *The Journal of Chemical Thermodynamics*, vol. 77, pp. 31–39, 2014.

[41] A. P. Fröba, H. Kremer, and A. Leipertz, "Density, refractive index, interfacial tension, and viscosity of ionic liquids [EMIM] [$EtSO_4$], [EMIM] [NTf_2], [EMIM] [$N(CN)_2$], and [OMA] [NTf_2] in dependence on temperature at atmospheric pressure," *The Journal of Physical Chemistry B*, vol. 112, no. 39, Article ID 12420, 2008.

[42] Y. Paulechka, A. Blokhin, G. J. Kabo, and A. A. Strechan, "Thermodynamic properties and polymorphism of 1-alkyl-3-methylimidazolium bis(triflamides)," *The Journal of Chemical Thermodynamics*, vol. 39, no. 6, pp. 866–877, 2007.

[43] M. Dzida, M. Chorążewski, M. Geppert-Rybczyńska et al., "Speed of sound and adiabatic compressibility of 1-ethyl-3-methylimidazolium bis(trifluoromethylsulfonyl)imide under pressures up to 100 MPa," *Journal of Chemical & Engineering Data*, vol. 58, no. 6, pp. 1571–1576, 2013.

[44] C. P. Fredlake, J. M. Crosthwaite, D. G. Hert, S. N. V. K. Aki, and J. F. Brennecke, "Thermophysical properties of imidazolium-based ionic liquids," *Journal of Chemical & Engineering Data*, vol. 49, no. 4, pp. 954–964, 2004.

[45] M. G. Freire, A. R. R. Teles, M. A. A. Rocha et al., "Thermophysical characterization of ionic liquids able to dissolve biomass," *Journal of Chemical & Engineering Data*, vol. 56, no. 12, pp. 4813–4822, 2011.

[46] G. García-Miaja, J. Troncoso, and L. Romaní, "Excess properties for binary systems ionic liquid+ethanol: experimental results and theoretical description using the ERAS model," *Fluid Phase Equilibria*, vol. 274, no. 1-2, pp. 59–67, 2008.

[47] G. García-Miaja, J. Troncoso, and L. Romaní, "Excess molar properties for binary systems of alkylimidazolium-based ionic liquids+nitromethane. Experimental results and ERAS-model calculations," *The Journal of Chemical Thermodynamics*, vol. 41, no. 3, pp. 334–341, 2009.

[48] A. Diedrichs and J. Gmehling, "Measurement of heat capacities of ionic liquids by differential scanning calorimetry," *Fluid Phase Equilibria*, vol. 244, no. 1, pp. 68–77, 2006.

[49] H. Schmidt, M. Stephan, J. Safarov et al., "Experimental study of the density and viscosity of 1-ethyl-3-methylimidazolium ethyl sulfate," *The Journal of Chemical Thermodynamics*, vol. 47, pp. 68–75, 2012.

[50] D. Matkowska, A. Goldon, and T. Hofman, "Densities, excess volumes, isobaric expansivities, and isothermal compressibilities of the 1-Ethyl-3-methylimidazolium ethylsulfate + ethanol system at temperatures (283.15 to 343.15) K and pressures from (0.1 to 35) MPa," *Journal of Chemical & Engineering Data*, vol. 55, no. 2, pp. 685–693, 2010.

[51] Z. H. Zhang, Z. C. Tan, L. X. Sun, Y. Jia-Zhen, X. C. Lv, and Q. Shi, "Thermodynamic investigation of room temperature ionic liquid: the heat capacity and standard enthalpy of formation of EMIES," *Thermochimica Acta*, vol. 447, no. 2, pp. 141–146, 2006.

[52] J. Palgunadi, J. E. Kang, D. Q. Nguyen et al., "Solubility of CO_2 in dialkylimidazolium dialkylphosphate ionic liquids," *Thermochimica Acta*, vol. 494, no. 1-2, pp. 94–98, 2009.

[53] J. Y. Wang, F. Y. Zhao, R. J. Liu, and Y. Q. Hu, "Thermophysical properties of 1-methyl-3-methylimidazolium dimethylphosphate and 1-ethyl-3-methylimidazolium diethylphosphate," *The Journal of Chemical Thermodynamics*, vol. 43, no. 1, pp. 47–50, 2011.

[54] C. M. Tenney, M. Massel, J. M. Mayes, M. Sen, J. F. Brennecke, and E. J. Maginn, "A computational and experimental study of the heat transfer properties of nine different ionic liquids," *Journal of Chemical & Engineering Data*, vol. 59, no. 2, pp. 391–399, 2014.

[55] J. Jacquemin, P. Husson, V. Majer, and M. F. C. Gomes, "Low-pressure solubilities and thermodynamics of solvation of eight gases in 1-butyl-3-methylimidazolium hexafluorophosphate," *Fluid Phase Equilibria*, vol. 240, no. 1, pp. 87–95, 2006.

[56] R. L. Gardas, M. G. Freire, P. J. Carvalho et al., "High-pressure densities and derived thermodynamic properties of imidazolium-based ionic liquids," *Journal of Chemical & Engineering Data*, vol. 52, no. 1, pp. 80–88, 2007.

[57] Y. J. Xu, Y. Huang, B. Wu, X. P. Zhang, and S. J. Zhang, "Biogas upgrading technologies: energetic analysis and environmental impact assessment," *Chinese Journal of Chemical Engineering*, vol. 23, no. 1, pp. 247–254, 2015.

[58] X. P. Zhang, X. Z. He, and T. Gundersen, "Post-combustion carbon capture with a gas separation membrane: parametric study, capture cost, and exergy analysis," *Energy and Fuels*, vol. 27, no. 8, pp. 4137–4149, 2013.

[59] A. N. Soriano, B. T. Doma Jr, and M. H. Li, "Measurements of the density and refractive index for 1-n-butyl-3-methylimidazolium-based ionic liquids," *The Journal of Chemical Thermodynamics*, vol. 41, no. 3, pp. 301–307, 2009.

[60] J. Troncoso, C. A. Cerdeirina, Y. A. Sanmamed, L. Romani, and L. P. N. Rebelo, "Thermodynamic properties of imidazolium-based ionic liquids: densities, heat capacities, and enthalpies of fusion of [bmim] [PF_6] and [bmim]

[NTf_2],” *Journal of Chemical & Engineering Data*, vol. 51, no. 5, pp. 1856–1859, 2006.

[61] J. Zhang, Q. H. Zhang, B. T. Qiao, and Y. Q. Deng, “Solubilities of the gaseous and liquid solutes and their thermodynamics of solubilization in the novel room-temperature ionic liquids at infinite dilution by gas chromatography,” *Journal of Chemical & Engineering Data*, vol. 52, no. 6, pp. 2277–2283, 2007.

[62] C. A. Nieto de Castro, E. Langa, A. L. Morais et al., “Studies on the density, heat capacity, surface tension and infinite dilution diffusion with the ionic liquids [C_4mim] [NTf_2], [C_4mim] [dca], [C_2mim] [$EtOSO_3$] and [Aliquat] [dca],” *Fluid Phase Equilibria*, vol. 294, no. 1-2, pp. 157–179, 2010.

[63] P. J. Carvalho, T. Regueira, L. M. N. B. F. Santos, J. Fernandez, and J. A. P. Coutinho, “Effect of water on the viscosities and densities of 1-butyl-3-methylimidazolium dicyanamide and 1-butyl-3-methylimidazolium tricyanomethane at atmospheric pressure,” *Journal of Chemical & Engineering Data*, vol. 55, no. 2, pp. 645–652, 2010.

[64] P. Navarro, M. Larriba, E. Rojo, J. Garcia, and F. Rodriguez, “Thermal properties of cyano-based ionic liquids,” *Journal of Chemical & Engineering Data*, vol. 58, no. 8, pp. 2187–2193, 2013.

[65] H. Tokuda, S. Tsuzuki, M. A. B. H. Susan, K. Hayamizu, and M. Watanabe, “How ionic are room-temperature ionic liquids? An indicator of the physicochemical properties,” *The Journal of Physical Chemistry B*, vol. 110, no. 39, Article ID 19593, 2006.

[66] A. A. Strechan, Y. U. Paulechka, A. V. Blokhin, and G. J. Kabo, “Low-temperature heat capacity of hydrophilic ionic liquids [BMIM] [CF_3COO] and [BMIM] [CH_3COO] and a correlation scheme for estimation of heat capacity of ionic liquids,” *The Journal of Chemical Thermodynamics*, vol. 40, no. 4, pp. 632–639, 2008.

[67] A. A. Miran Beigi, M. Abdouss, M. Yousefi, S. M. Pourmortazavi, and A. Vahid, “Investigation on physical and electrochemical properties of three imidazolium based ionic liquids (1-hexyl-3-methylimidazolium tetrafluoroborate, 1-ethyl-3-methylimidazolium bis(trifluoromethylsulfonyl) imide and 1-butyl-3-methylimidazolium methylsulfate),” *Journal of Molecular Liquids*, vol. 177, pp. 361–368, 2013.

[68] Y. H. Yu, A. N. Soriano, and M. H. Li, “Heat capacities and electrical conductivities of 1-n-butyl-3-methylimidazolium-based ionic liquids,” *Thermochimica Acta*, vol. 482, no. 1-2, pp. 42–48, 2009.

[69] M. J. Davila, S. Aparicio, R. Alcalde, B. Garcia, and J. M. Leal, “On the properties of 1-butyl-3-methylimidazolium octylsulfate ionic liquid,” *Green Chemistry*, vol. 9, no. 3, pp. 221–232, 2007.

[70] J. H. Yim and J. S. Lim, “CO_2 solubility measurement in 1-hexyl-3-methylimidazolium ([HMIM]) cation based ionic liquids,” *Fluid Phase Equilibria*, vol. 352, pp. 67–74, 2013.

[71] Y. A. Sanmamed, D. González-Salgado, J. Troncoso, C. A. Cerdeiriña, and L. Romaní, “Viscosity-induced errors in the density determination of room temperature ionic liquids using vibrating tube densitometry,” *Fluid Phase Equilibria*, vol. 252, no. 1–2, pp. 96–102, 2007.

[72] D. Waliszewski, “Heat capacities of the mixtures of ionic liquids with methanol at temperatures from 283.15 K to 323.15 K,” *The Journal of Chemical Thermodynamics*, vol. 40, no. 2, pp. 203–207, 2008.

[73] G. Vakili-Nezhaad, M. Vatani, M. Asghari, and I. Ashour, “Effect of temperature on the physical properties of 1-butyl-3-methylimidazolium based ionic liquids with thiocyanate and tetrafluoroborate anions, and 1-hexyl-3-methylimidazolium with tetrafluoroborate and hexafluorophosphate anions,” *The Journal of Chemical Thermodynamics*, vol. 54, pp. 148–154, 2012.

[74] J. G. Li, Y. F. Hu, S. Ling, and J. Z. Zhang, “Physicochemical properties of [C_6mim] [PF_6] and [C_6mim] [$(C_2F_5)_3PF_3$] ionic liquids,” *Journal of Chemical & Engineering Data*, vol. 56, no. 7, pp. 3068–3072, 2011.

[75] J. Kumelan, Á. Pérez-Salado Kamps, D. Tuma, and G. Maurer, “Solubility of CO_2 in the ionic liquid [hmim] [Tf_2N],” *The Journal of Chemical Thermodynamics*, vol. 38, no. 11, pp. 1396–1401, 2006.

[76] J. A. Widegren and J. W. Magee, “Density, viscosity, speed of sound, and electrolytic conductivity for the ionic liquid 1-hexyl-3-methylimidazolium bis(trifluoromethylsulfonyl) imide and its mixtures with water,” *Journal of Chemical & Engineering Data*, vol. 52, no. 6, pp. 2331–2338, 2007.

[77] Y. U. Paulechka, A. V. Blokhin, and G. J. Kabo, “Evaluation of thermodynamic properties for non-crystallizable ionic liquids,” *Thermochimica Acta*, vol. 604, pp. 122–128, 2015.

[78] V. H. Alvarez and M. D. A. Saldaña, “Thermodynamic prediction of vapor–liquid equilibrium of supercritical CO_2 or CHF_3 + ionic liquids,” *The Journal of Supercritical Fluids*, vol. 66, pp. 29–35, 2012.

[79] M. A. A. Rocha, M. Bastos, J. A. P. Coutinho, and L. M. N. B. F. Santos, “Heat capacities at 298.15 K of the extended [$C(_n)C(_1)$im] [$NTf(_2)$] ionic liquid series,” *The Journal of Chemical Thermodynamics*, vol. 53, pp. 140–143, 2012.

[80] F. M. Gacino, T. Regueira, L. Lugo, M. J. P. Comunas, and J. Fernandez, “Influence of molecular structure on densities and viscosities of several ionic liquids,” *Journal of Chemical & Engineering Data*, vol. 56, no. 12, pp. 4984–4999, 2011.

[81] R. L. Gardas, H. F. Costa, M. G. Freire et al., “Densities and derived thermodynamic properties of imidazolium-pyridinium-pyrrolidinium-and piperidinium-based ionic liquids,” *Journal of Chemical & Engineering Data*, vol. 53, no. 3, pp. 805–811, 2008.

[82] E. J. Gonzalez, A. Dominguez, and E. A. Macedo, “Physical and excess properties of eight binary mixtures containing water and ionic liquids,” *Journal of Chemical & Engineering Data*, vol. 57, no. 8, pp. 2165–2176, 2012.

[83] N. M. Yunus, M. A. Mutalib, Z. Man, M. A. Bustam, and T. Murugesan, “Solubility of CO_2 in pyridinium based ionic liquids,” *Chemical Engineering Journal*, vol. 189, no. 0, pp. 94–100, 2012.

[84] F. S. Oliveira, M. G. Freire, P. J. Carvalho et al., “Structural and positional isomerism influence in the physical properties of pyridinium NTf_2-based ionic liquids: pure and water-saturated mixtures,” *Journal of Chemical & Engineering Data*, vol. 55, no. 10, pp. 4514–4520, 2010.

[85] Q. S. Liu, P. P. Li, U. Welz-Biermann, J. Chen, and X. X. Liu, “Density, dynamic viscosity, and electrical conductivity of pyridinium-based hydrophobic ionic liquids,” *The Journal of Chemical Thermodynamics*, vol. 66, pp. 88–94, 2013.

[86] J. M. Crosthwaite, M. J. Muldoon, J. K. Dixon, J. L. Anderson, and J. F. Brennecke, “Phase transition and decomposition temperatures, heat capacities and viscosities of pyridinium ionic liquids,” *The Journal of Chemical Thermodynamics*, vol. 37, no. 6, pp. 559–568, 2005.

[87] P. Kilaru, G. A. Baker, and P. Scovazzo, “Density and surface tension measurements of imidazolium-quaternaryphosphonium-andammonium-basedroom-temperature ionic liquids: data and

correlations," *Journal of Chemical & Engineering Data*, vol. 52, no. 6, pp. 2306–2314, 2007.

[88] Y. U. Paulechka, A. G. Kabo, A. V. Blokhin, G. J. Kabo, and M. P. Shevelyova, "Heat capacity of ionic liquids: experimental determination and correlations with molar volume," *Journal of Chemical & Engineering Data*, vol. 55, no. 8, pp. 2719–2724, 2010.

[89] X. Y. Li, M. Q. Hou, B. X. Han, X. L. Wang, and L. Z. Zou, "Solubility of CO_2 in a choline chloride + urea eutectic mixture," *Journal of Chemical & Engineering Data*, vol. 53, no. 2, pp. 548–550, 2008.

[90] O. Ciocirlan, O. Iulian, and O. Croitoru, "Effect of temperature on the physico-chemical properties of three ionic liquids containing choline chloride," *Revista de Chimie*, vol. 61, no. 8, pp. 721–723, 2010.

[91] R. B. Leron and M. H. Li, "High-pressure density measurements for choline chloride: urea deep eutectic solvent and its aqueous mixtures at T = (298.15 to 323.15) K and up to 50 MPa," *The Journal of Chemical Thermodynamics*, vol. 54, pp. 293–301, 2012.

[92] A. Bakhtyari, R. Haghbakhsh, A. R. C. Duarte, and S. Raeissi, "A simple model for the viscosities of deep eutectic solvents," *Fluid Phase Equilibria*, vol. 521, Article ID 112662, 2020.

[93] R. B. Leron and M. H. Li, "Molar heat capacities of choline chloride-based deep eutectic solvents and their binary mixtures with water," *Thermochimica Acta*, vol. 530, pp. 52–57, 2012.

[94] R. B. Leron and M. H. Li, "Solubility of carbon dioxide in a choline chloride–ethylene glycol based deep eutectic solvent," *Thermochimica Acta*, vol. 551, pp. 14–19, 2013.

[95] R. B. Leron, A. N. Soriano, and M. H. Li, "Densities and refractive indices of the deep eutectic solvents (choline chloride + ethylene glycol or glycerol) and their aqueous mixtures at the temperature ranging from 298.15 to 333.15 K," *Journal of the Taiwan Institute of Chemical Engineers*, vol. 43, no. 4, pp. 551–557, 2012.

[96] R. B. Leron and M. H. Li, "Solubility of carbon dioxide in a eutectic mixture of choline chloride and glycerol at moderate pressures," *The Journal of Chemical Thermodynamics*, vol. 57, pp. 131–136, 2013.

[97] R. B. Leron, D. S. H. Wong, and M. H. Li, "Densities of a deep eutectic solvent based on choline chloride and glycerol and its aqueous mixtures at elevated pressures," *Fluid Phase Equilibria*, vol. 335, pp. 32–38, 2012.

[98] H. F. D. Almeida, H. Passos, J. A. Lopes-da-Silva, A. M. Fernandes, M. G. Freire, and J. A. P. Coutinho, "Thermophysical properties of five acetate-based ionic liquids," *Journal of Chemical & Engineering Data*, vol. 57, no. 11, pp. 3005–3013, 2012.

[99] C. Su, X. Y. Liu, C. Y. Zhu, and M. G. He, "Isobaric molar heat capacities of 1-ethyl-3-methylimidazolium acetate and 1-hexyl-3-methylimidazolium acetate up to 16 MPa," *Fluid Phase Equilibria*, vol. 427, pp. 187–193, 2016.

[100] M. B. Shiflett, B. A. Elliott, S. R. Lustig, S. Sabesan, M. S. Kelkar, and A. Yokozeki, "Phase behavior of CO_2 in room-temperature ionic liquid 1-ethyl-3-ethylimidazolium acetate," *ChemPhysChem*, vol. 13, no. 7, pp. 1806–1817, 2012.

[101] M. B. Shiflett, D. J. Kasprzak, C. P. Junk, and A. Yokozeki, "Phase behavior of {carbon dioxide+[bmim] [Ac]} mixtures," *The Journal of Chemical Thermodynamics*, vol. 40, no. 1, pp. 25–31, 2008.

[102] Y. F. Chen, Y. Y. Zhang, S. J. Yuan et al., "Thermodynamic study for CO_2 absorption in (2-hydroxyethyl)-trimethyl -ammonium(S)-2-pyrrolidinecarboxylic acid salt + polyethylene glycol," *Journal of Chemical & Engineering Data*, vol. 61, no. 10, pp. 3428–3437, 2016.

[103] Y. F. Chen, Y. H. Sun, Z. H. Yang, X. H. Lu, and X. Y. Ji, "CO_2 separation using a hybrid choline-2-pyrrolidine-carboxylic acid/polyethylene glycol/water absorbent," *Applied Energy*, vol. 257, Article ID 113962, 2020.

[104] S. Stevanovic and M. Costa Gomes, "Solubility of carbon dioxide, nitrous oxide, ethane and nitrogen in 1-butyl-1-methylpyrrolidinium and trihexyl(tetradecyl)phosphonium tris(pentafluoroethyl)trifluorophosphate (eFAP) ionic liquids," *The Journal of Chemical Thermodynamics*, vol. 59, pp. 65–71, 2013.

[105] M. Vraneš, A. Tot, N. Zec, S. Papović, and S. Gadžurić, "Volumetric properties of binary mixtures of 1-butyl-1-methylpyrrolidinium tris (pentafluoroethyl) trifluorophosphate with N-methylformamide, N-ethylformamide, N, N-dimethylformamide, N, N-dibutylformamide, and N, N-dimethylacetamide from (293.15 to 323.15) K," *Journal of Chemical and Engineering Data*, vol. 12, no. 3, pp. 441–446, 2014.

[106] R. Ge, C. Hardacre, J. Jacquemin, P. Nancarrow, and D. W. Rooney, "Heat capacities of ionic liquids as a function of temperature at 0.1 MPa. measurement and prediction," *Journal of Chemical & Engineering Data*, vol. 53, no. 9, pp. 2148–2153, 2008.

[107] A. F. Ferreira, P. N. SimõEs, and A. G. Ferreira, "Quaternary phosphonium-based ionic liquids: thermal stability and heat capacity of the liquid phase," *The Journal of Chemical Thermodynamics*, vol. 45, no. 1, pp. 16–27, 2012.

[108] D. Almantariotis, S. Stevanovic, O. Fandiño et al., "Absorption of carbon dioxide, nitrous oxide, ethane and nitrogen by 1-Alkyl-3-methylimidazolium ($c_n$mim, n = 2,4,6) tris(pentafluoroethyl)trifluorophosphate ionic liquids (eFAP)," *The Journal of Physical Chemistry B*, vol. 116, no. 26, pp. 7728–7738, 2012.

[109] J. Safarov, F. Lesch, K. Suleymanli et al., "High-temperature and high-pressure density measurements and other derived thermodynamic properties of 1-butyl-3-methylimidazolium tris (pentafluoroethyl) trifluorophosphate," *Thermochimica Acta*, vol. 658, pp. 14–23, 2017.

[110] J. Safarov, F. Lesch, K. Suleymanli et al., "Viscosity, density, heat capacity, speed of sound and other derived properties of 1-butyl-3-methylimidazolium tris(pentafluoroethyl) trifluorophosphate over a wide range of temperature and at atmospheric pressure," *Journal of Chemical & Engineering Data*, vol. 62, no. 10, pp. 3620–3631, 2017.

[111] M. Součková, J. Klomfar, and J. Pátek, "Temperature dependence of the surface tension and 0.1 MPa density for 1-Cn-3-methylimidazolium tris(pentafluoroethyl)trifluorophosphate with n = 2, 4, and 6," *The Journal of Chemical Thermodynamics*, vol. 48, no. 1, pp. 267–275, 2012.

[112] M. B. Shiflett, A. M. S. Niehaus, B. A. Elliott, and A. Yokozeki, "Phase behavior of N_2O and CO_2 in room-temperature ionic liquids [bmim] [Tf_2N], [bmim] [BF_4], [bmim] [$N(CN)_2$], [bmim] [Ac], [eam] [NO_3], and [bmim] [SCN]," *International Journal of Thermophysics*, vol. 33, no. 3, pp. 412–436, 2012.

[113] J. Salg Ad O, T. Regueira, L. Lugo, J. Vijande, J. Fernández, and J. García, "Density and viscosity of three (2,2,2-trifluoroethanol + 1-butyl-3-methylimidazolium) ionic liquid binary systems," *The Journal of Chemical Thermodynamics*, vol. 70, pp. 101–110, 2014.

[114] R. Hamidova, I. Kul, J. Safarov, A. Shahverdiyev, and E. Hassel, "Thermophysical properties of 1-butyl-3-

methylimidazolium bis(trifluoromethylsulfonyl)imide at high temperatures and pressures," *Brazilian Journal of Chemical Engineering*, vol. 32, no. 1, pp. 303–316, 2015.

[115] D. Matkowska and T. Hofman, "High-pressure volumetric properties of ionic liquids: 1-butyl-3-methylimidazolium tetrafluoroborate, [C_4mim] [BF_4], 1-butyl-3-methylimidazolium methylsulfate [C_4mim] [$MeSO_4$] and 1-ethyl-3-methylimidazolium ethylsulfate, [C_2mim] [$EtSO_4$]," *Journal of Molecular Liquids*, vol. 165, pp. 161–167, 2012.

[116] N. Calvar, E. Gómez, E. A. Macedo, and Á. Domínguez, "Thermal analysis and heat capacities of pyridinium and imidazolium ionic liquids," *Thermochimica Acta*, vol. 565, pp. 178–182, 2013.

[117] J. Safarov, M. Geppert-Rybczyńska, I. Kul, and E. Hassel, "Thermophysical properties of 1-butyl-3-methylimidazolium acetate over a wide range of temperatures and pressures," *Fluid Phase Equilibria*, vol. 383, pp. 144–155, 2014.

[118] E. Zorebski, M. Musiał, K. Baluszynska, M. Zorebski, and M. Dzida, "Isobaric and isochoric heat capacities as well as isentropic and isothermal compressibilities of di- and trisubstituted imidazolium-based ionic liquids as a function of temperature," *Industrial & Engineering Chemistry Research*, vol. 57, no. 14, pp. 5161–5172, 2018.

[119] A. H. Jalili, M. Rahmati-Rostami, C. Ghotbi, M. Hosseini-Jenab, and A. N. Ahmadi, "Solubility of H_2S in ionic liquids [bmim] [PF_6], [bmim] [BF_4], and [bmim] [Tf_2N]," *Journal of Chemical & Engineering Data*, vol. 54, no. 6, pp. 1844–1849, 2009.

[120] M. Safavi, C. Ghotbi, V. Taghikhani, A. H. Jalili, and A. Mehdizadeh, "Study of the solubility of CO_2, H_2S and their mixture in the ionic liquid 1-octyl-3-methylimidazolium hexafluorophosphate: experimental and modelling," *The Journal of Chemical Thermodynamics*, vol. 65, pp. 220–232, 2013.

[121] N. Zhang, T. L. Deng, and M. M. Liu, "Synthesis and physicochemical properties of ionic liquids [Bmim]Br and [Bmim]PF_6," *Journal of Tianjin University of Science & Technology*, vol. 29, no. 05, pp. 42–47, 2014.

[122] M. Rahmati-Rostami, C. Ghotbi, M. Hosseini-Jenab, A. N. Ahmadi, and A. H. Jalili, "Solubility of H_2S in ionic liquids [hmim] [PF_6], [hmim] [BF_4], and [hmim] [Tf_2N]," *The Journal of Chemical Thermodynamics*, vol. 41, no. 9, pp. 1052–1055, 2009.

[123] O. Iulian and O. Ciocirlan, "Volumetric properties of binary mixtures of two 1-alkyl-3-methylimidazolium tetrafluoroborate ionic liquids with molecular solvents," *Journal of Chemical & Engineering Data*, vol. 57, no. 10, pp. 2640–2646, 2012.

[124] M. A. A. Rocha, F. M. S. Ribeiro, A. I. L. Ferreira, J. A. P. Coutinho, and L. M. Santos, "Thermophysical properties of [$C_{N\text{-}1}C_1$im] [PF_6] ionic liquids[J]," *Journal of Molecular Liquids*, vol. 188, pp. 196–202, 2013.

[125] P. B. P. Serra, F. M. S. Ribeiro, M. A. A. Rocha et al., "Solid-liquid equilibrium and heat capacity trend in the alkylimidazolium PF_6 series[J]," *Journal of Molecular Liquids*, vol. 248, pp. 678–687, 2017.

[126] R. G. D. Azevedo, J. Esperanca, J. Szydlowski et al., "Thermophysical and thermodynamic properties of ionic liquids over an extended pressure range: [bmim][NTf_2] and [hmim][NTf_2]," *Journal of Chemical Thermodynamics*, vol. 37, no. 9, pp. 888–899, 2005.

[127] Y. Shimizu, Y. Ohte, Y. Yamamura, K. Saito, and T. Atake, "Low-temperature heat capacity of room-temperature ionic liquid, 1-Hexyl-3-methylimidazolium bis(trifluoromethylsulfonyl)imide," *The Journal of Physical Chemistry B*, vol. 110, no. 28, pp. 13970–13975, 2006.

[128] H. Sakhaeinia, A. H. Jalili, V. Taghikhani, and A. A. Safekordi, "Solubility of H_2S in ionic liquids 1-ethyl-3-methylimidazolium hexafluorophosphate ([emim] [PF_6]) and 1-ethyl-3-methylimidazolium bis(trifluoromethyl)sulfonylimide ([emim] [Tf_2N])," *Journal of Chemical & Engineering Data*, vol. 55, no. 12, pp. 5839–5845, 2010.

[129] A. H. Jalili, A. Mehdizadeh, M. Shokouhi, A. N. Ahmadi, M. Hosseini-Jenab, and F. Fateminassab, "Solubility and diffusion of CO_2 and H_2S in the ionic liquid 1-ethyl-3-methylimidazolium ethylsulfate," *The Journal of Chemical Thermodynamics*, vol. 42, no. 10, pp. 1298–1303, 2010.

[130] G. García-Miaja, J. Troncoso, and L. Romani, "Excess enthalpy, density, and heat capacity for binary systems of alkylimidazolium-based ionic liquids+water," *The Journal of Chemical Thermodynamics*, vol. 41, no. 2, pp. 161–166, 2009.

[131] A. H. Jalili, M. Safavi, C. Ghotbi, A. Mehdizadeh, M. Hosseini-Jenab, and V. Taghikhani, "Solubility of CO_2, H_2S, and their mixture in the ionic liquid 1-octyl-3-methylimidazolium bis(trifluoromethyl)sulfonylimide," *The Journal of Physical Chemistry B*, vol. 116, no. 9, pp. 2758–2774, 2012.

[132] Z. J. Chen and J. M. Lee, "Free volume model for the unexpected effect of C2-methylation on the properties of imidazolium ionic liquids," *The Journal of Physical Chemistry B*, vol. 118, no. 10, pp. 2712–2718, 2014.

[133] Z. Vaid, U. More, S. P. Ijardar, and N. I. Malek, "Investigation on thermophysical and excess properties of binary mixtures of imidazolium based ionic liquids at temperatures (293.15 to 323.15)K: III [Cnmim] [PF_6] (n=4, 6, 8)+THF," *The Journal of Chemical Thermodynamics*, vol. 86, pp. 143–153, 2015.

[134] N. Dave, T. Do, D. Palfreyman, and P. Feron, "Impact of liquid absorption process development on the costs of post-combustion capture in Australian coal-fired power stations," *Chemical Engineering Research and Design*, vol. 89, no. 9, pp. 1625–1638, 2011.

[135] R. W. Bucklin and R. L. Schendel, "Comparison of fluor solvent and selexol processes," *Energy Progress*, vol. 4, pp. 137–142, 1984.

[136] D. Valencia-Marquez, A. Flores-Tlacuahuac, and L. Ricardez-Sandoval, "Technoeconomic and dynamical analysis of a CO_2 capture pilot-scale plant using ionic liquids," *Industrial & Engineering Chemistry Research*, vol. 54, no. 45, Article ID 11360, 2015.

[137] M. B. Shiflett, D. W. Drew, R. A. Cantini, and A. Yokozeki, "Carbon dioxide capture using ionic liquid 1-butyl-3-methylimidazolium acetate," *Energy and Fuels*, vol. 24, no. 10, pp. 5781–5789, 2010.

[138] A. M. Cormos, C. Dinca, and C. C. Cormos, "Energy efficiency improvements of post-combustion CO_2 capture based on reactive gas-liquid absorption applied for super-critical circulating fluidized bed combustion (CFBC) power plants," *Clean Technologies and Environmental Policy*, vol. 20, no. 6, pp. 1311–1321, 2018.